Cleavage Fracture in the Brittle to Ductile Transition: A Multiscale Approach

G. R Odette
Department of Mechanical and Environmental Engineering and
Department of Materials - UC Santa Barbara

P. Spätig (presenting author)
Centre de Recherches en Physique des Plasmas/EPF Lausanne

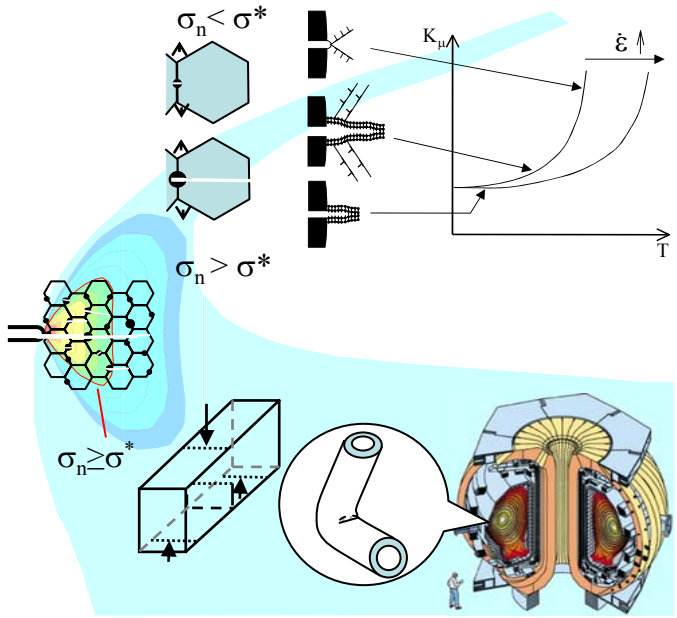

Research sponsored by US DOE and US NRC

Collaborators

M. Hribernik (UCSB)

M. He (UCSB)

H. Rathbun (UCSB)

T. Yamamoto (UCSB)

D. Klingensmith (UCSB)

D. Gragg (UCSB)

G. Lucas(UCSB)

W-J. Yang (UCSB-KAERI, Korea)

R. Yasuda (JAERI, Japan)

J-W. Rensman (NRG Petten, Netherlands)

Outline

- Focus on cleavage fracture in brittle to ductile (BDT) transition in bcc alloys:
  - characterize resistance to crack propagation by fracture toughness $K_{Jc}(T)$
  - apparent universal $K_{Jc}(T-T_o)$ curve shape
  - neutron embrittlement
  - size-geometry effects
  - measured toughness
  - statistical effects and intrinsic scatter

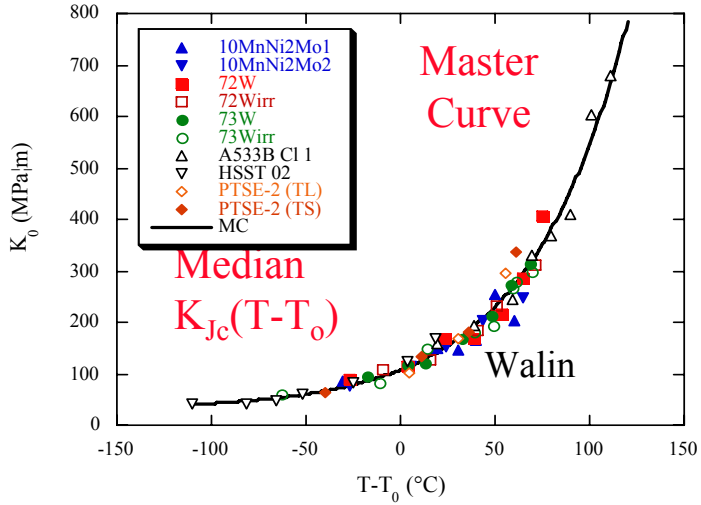

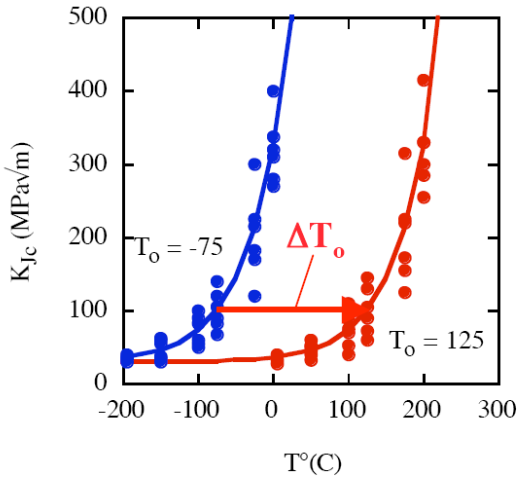

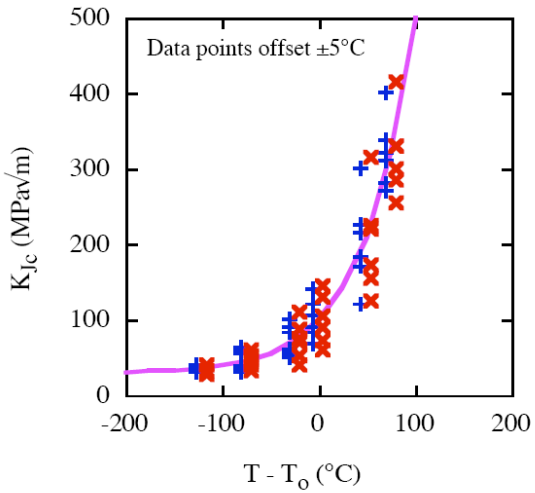

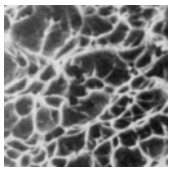

microvoid coalescence

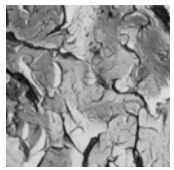

quasi-cleavage

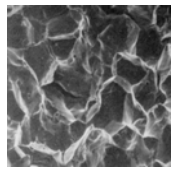

intergranular

transgranular cleavage

Fracture and Fracture Toughness

- Fracture - failure by crack propagation with damage => material separation in high σ–ε crack tip process zone

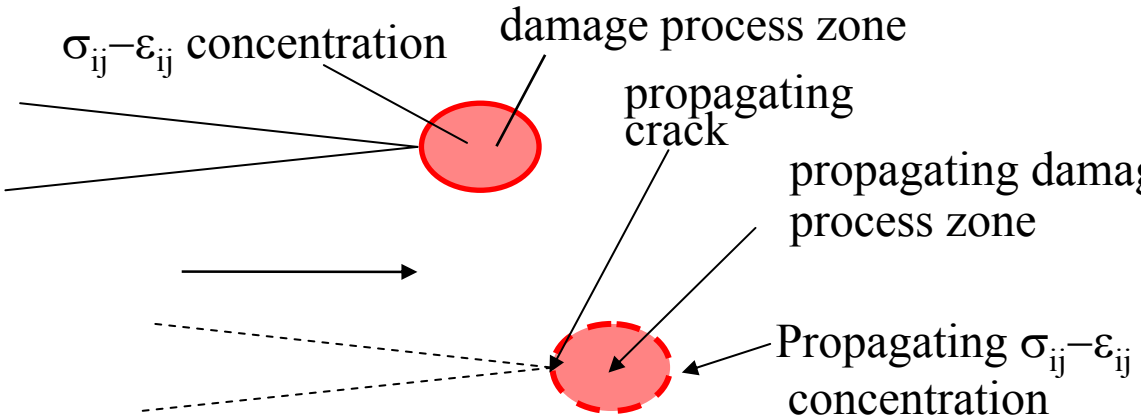

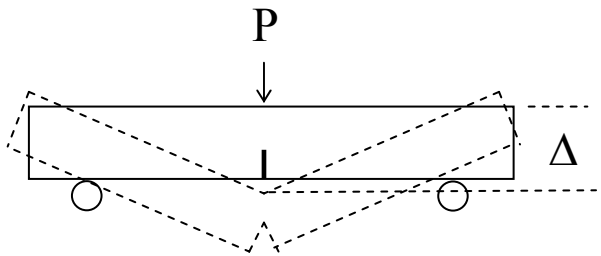

- Relate applied P(σ)-Δ(ε) => loading parameter like K_I => crack tip fields $\sigma_{ij}(r,\theta)$
- Coupon tests => *fracture toughness* K_{Ic}* fracture P(σ)-Δ(ε) in complex structures.

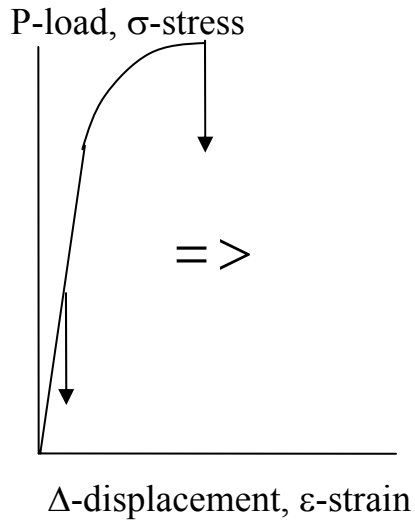

Linear Elastic Fracture Mechanic SIF

$K_I = \sigma_a f(\text{geometry})\sqrt{\text{crack length}}$

*many types

Classical Fracture Mechanics

- *Computable load parameter* - like elastic stress intensity factor K_I => characterize *crack tip **dominated*** fields

LEFM

$K_I^* = \sigma_a f(\text{geometry})\sqrt{\text{crack length}}$

K_I (structure at fracture) = K_{Ic} (coupon - material property)

$\sigma_f = [f(\text{geometry})K_{Ic}]/[\sqrt{\text{crack length}}]$

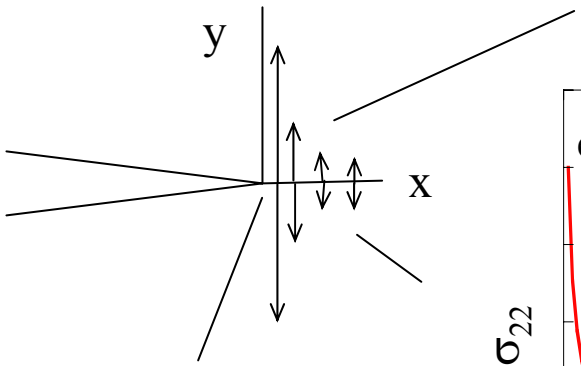

$\sigma_{22} = [K_I/(2\pi x)^{1/2}]$

*Mode 1 (opening)
plain strain
sharp fatigue crack

Same fields at same K_I and K_{Ic}

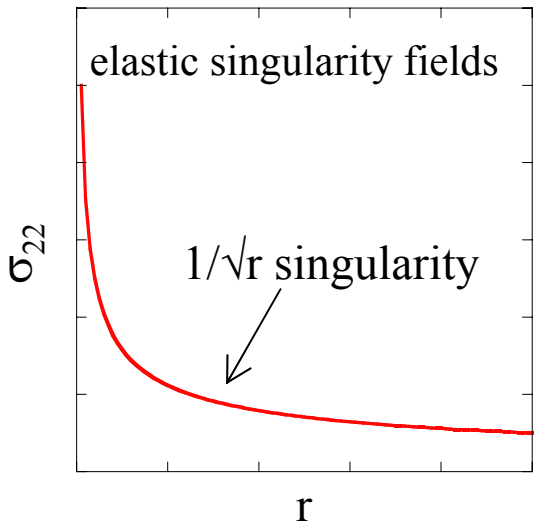

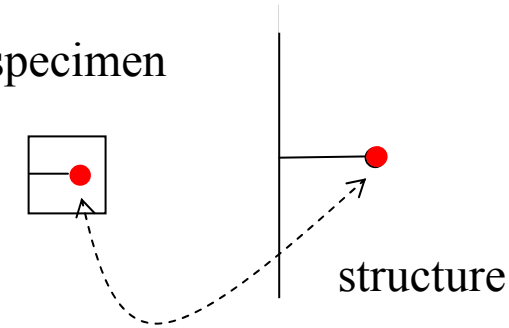

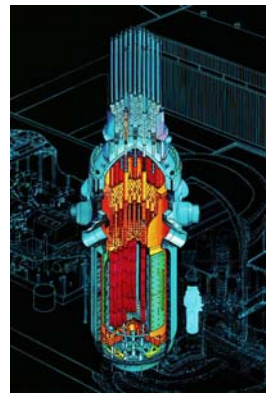

K_I versus K_{IC}

- K_I is like an applied stress in a tensile test - a measure of the loading on a cracked body
- K_{Ic} is like the yield stress in a tensile test - under limited conditions - it is a material "property" specifying the condition for crack propagation

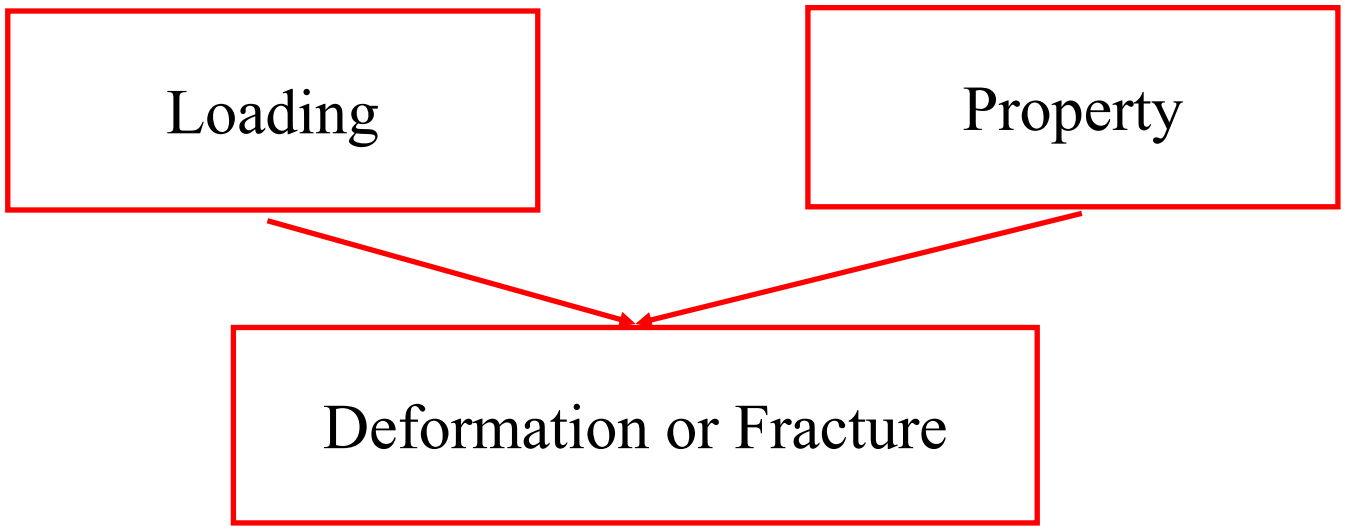

Elastic Fields and Stress Intensity Factor

Mode I

$$\sigma_{xx} \quad \frac{K_I}{\sqrt{2\pi r}}\cos\left(\frac{\theta}{2}\right)\left[1-\sin\left(\frac{\theta}{2}\right)\sin\left(\frac{3\theta}{2}\right)\right]$$

$$\sigma_{yy} \quad \frac{K_I}{\sqrt{2\pi r}}\cos\left(\frac{\theta}{2}\right)\left[1+\sin\left(\frac{\theta}{2}\right)\sin\left(\frac{3\theta}{2}\right)\right]$$

$$\tau_{xy} \quad \frac{K_I}{\sqrt{2\pi r}}\cos\left(\frac{\theta}{2}\right)\sin\left(\frac{\theta}{2}\right)\cos\left(\frac{3\theta}{2}\right)$$

σ_{zz} 0 (Plane stress)

$\nu(\sigma_{xx}+\sigma_{yy})$ (Plane strain)

τ_{xz}, τ_{yz} 0

Note: υ is Poisson's ratio.

SIF: $K_I = \dfrac{P}{B\sqrt{W}} f\left[\dfrac{a}{W}\right]$

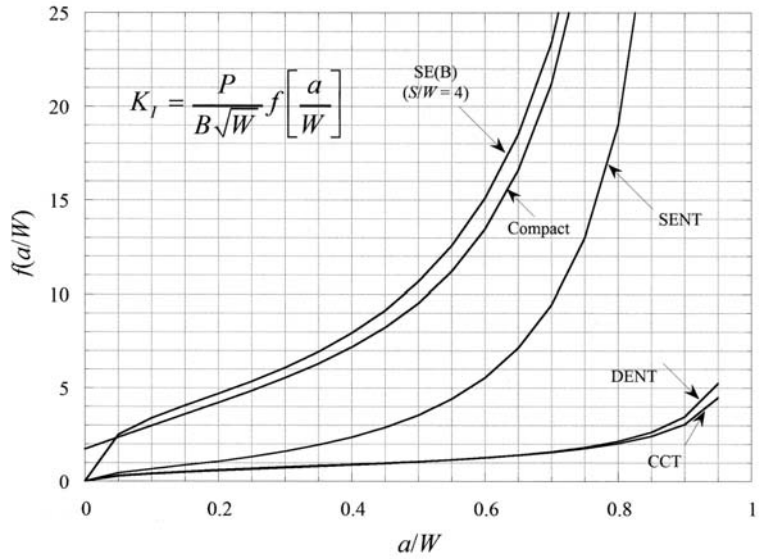

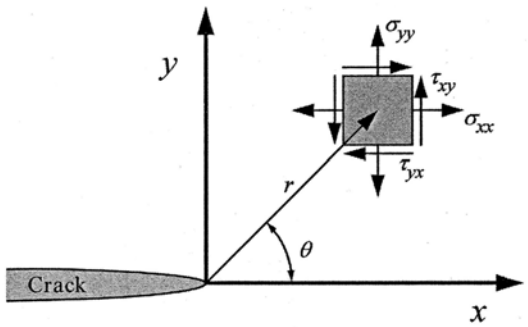

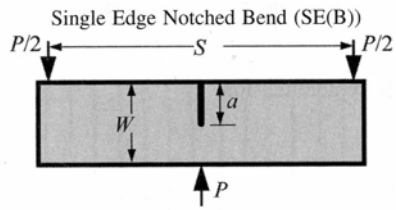

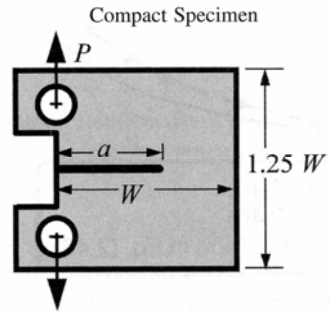

Effects of Plasticity

- Elastic fields occur only in most brittle materials
- Non-linear processes => plastic zone-blunting => reduce fields
- Measured-computed elastic-plastic
  K_J and δ still valid for *small scale yielding (SSY)*
  - small embedded plastic zones
  - deep cracks in bending
  - high strain hardening helps

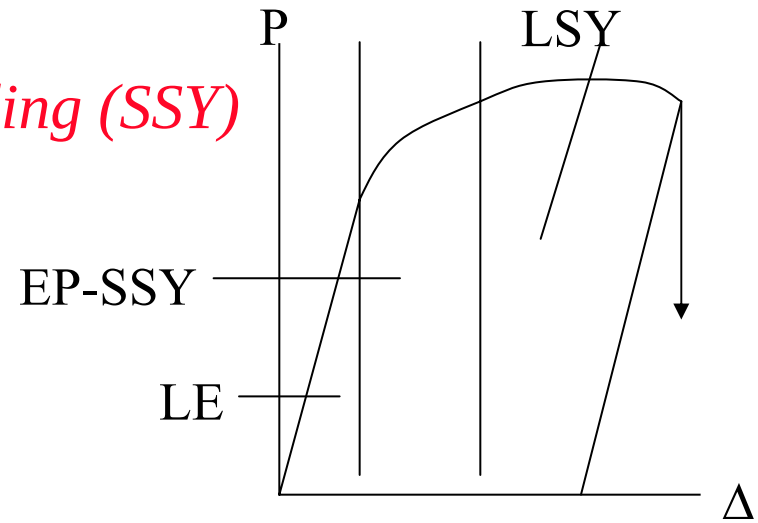

δ - crack tip opening displacement

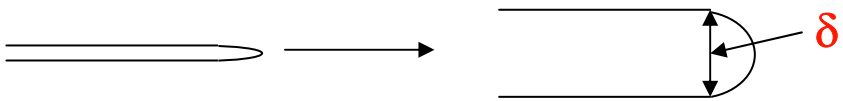

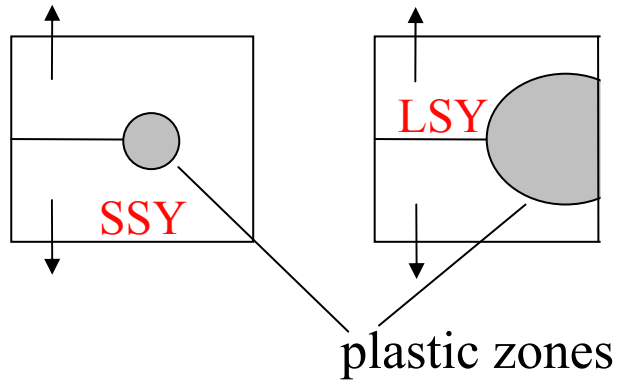

Fracture at: $K_J = K_{Jc}$ and $\delta = \delta_c$

K_{Jc}

- Elastic-plastic J-integral: $J \cong 2\sigma_y\delta$
- $K_J = [E'J]^{1/2}$
- $J = J_{el} + J_{pl}$
- $J_{el} = K_I^2/E' = f(a, P_e)$
- $J_{pl} = \eta A_{p\Delta}/bB$

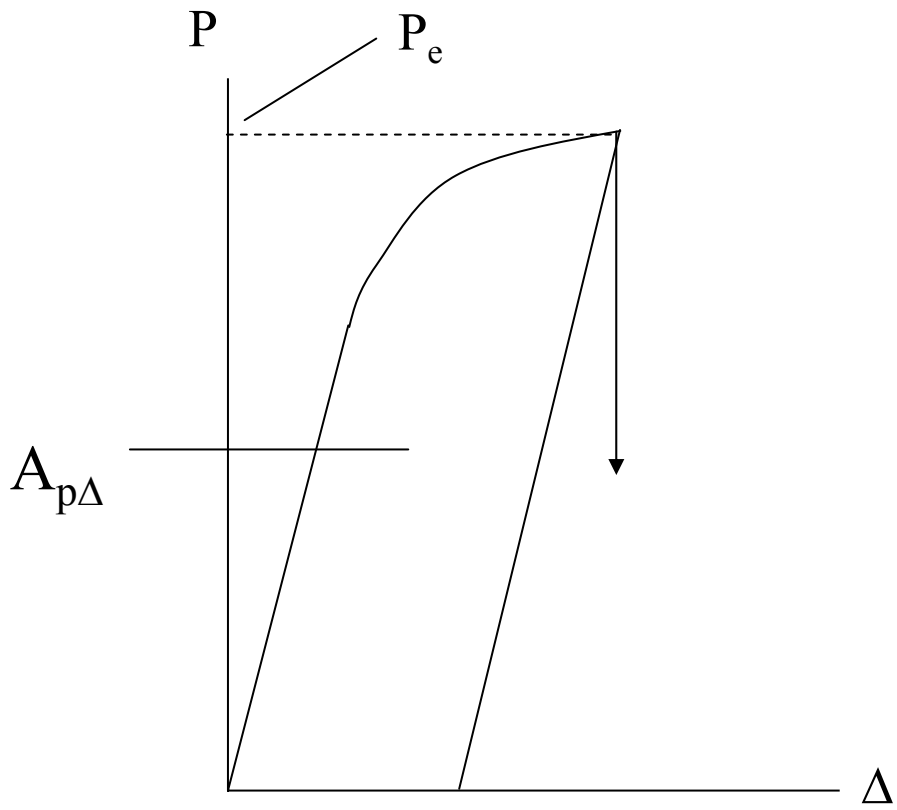

Small Scale Yielding (SSY) Fields

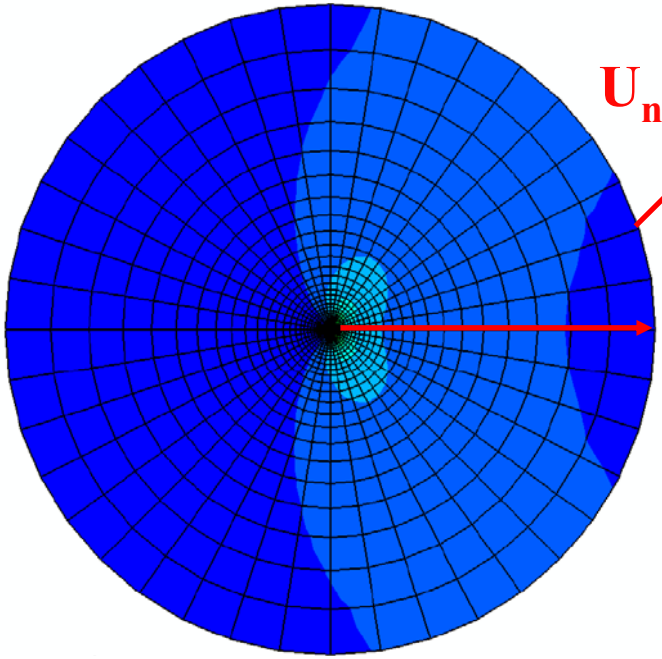

- Pure boundary layer model: stresses (and displacements) at the nodes on the boundary R_o are defined by K and θ only:

$$\sigma_{ij,boundary}(K,\theta) = \frac{K}{\sqrt{2\pi R_o}} f_{ij}(\theta)$$

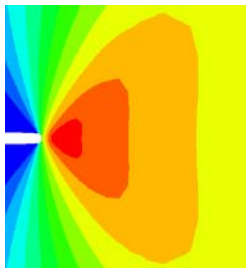

σ_{22} at the crack tip

Stress at any point: $\sigma_{ij} = \sigma_{ij}(r, \theta, K, \sigma_y, \sigma_{pl}(\varepsilon))$

Dimensional analysis and Buckingham theorem yield:

$$\sigma_{ij}/\sigma_y = [\sigma_{ij}(r/K^2/\sigma_y^2, \theta, \sigma_{pl}(\varepsilon)/\sigma_y)]/\sigma_y$$

Small Scale Yielding (SSY) Fields

- Deep cracks with T stress field = 0
- SSY fields - self-similar in r/δ ($\delta \approx 0.5K_J^2/\sigma_y E'$)
- The σ_{ij} stress fields and K_J functions of material $\sigma(\varepsilon, T, \varepsilon')$
- Finite element (FE) simulations of $\sigma_{ij}[r/\delta, \theta, \sigma(\varepsilon), \delta]$
- Peak σ_{22max}/σ_y = 3-5 for plane-ε SSY

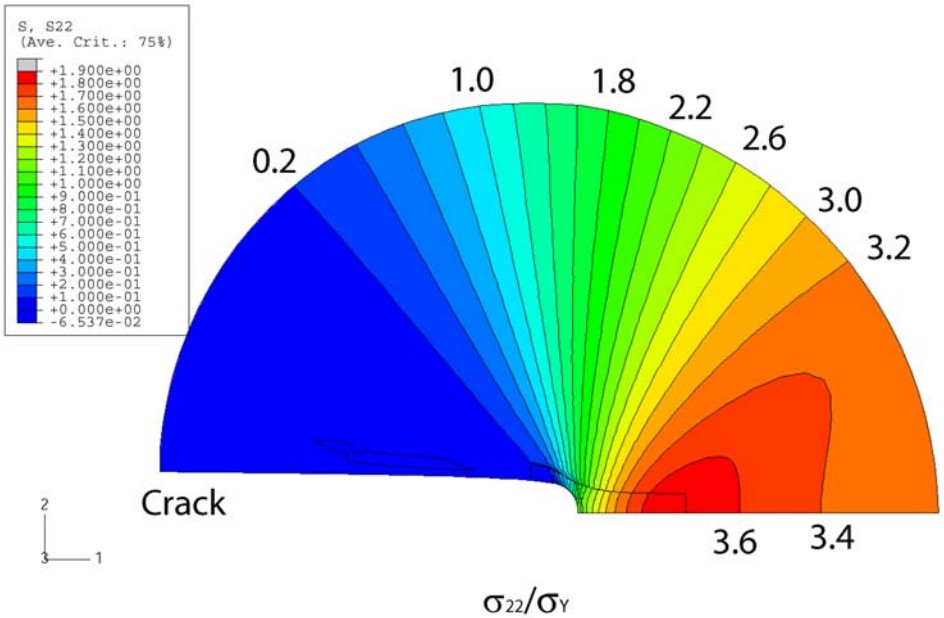

Constraint Effects - Tresca yielding @

$\sigma_{max} - \sigma_{min} > \sigma_y$

$\sigma_{max} >> \sigma_y$ for large σ_{min}

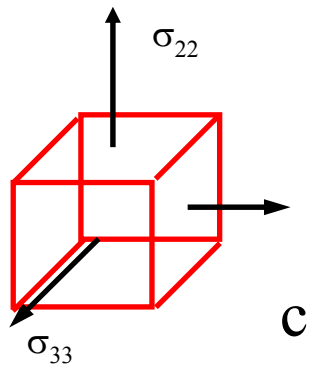

constraint

Small Scale Yielding (SSY) Fields

- High σ_{22} required for cleavage
- Critical $\sigma_{22} = \sigma^*$ over a critical volume - V*

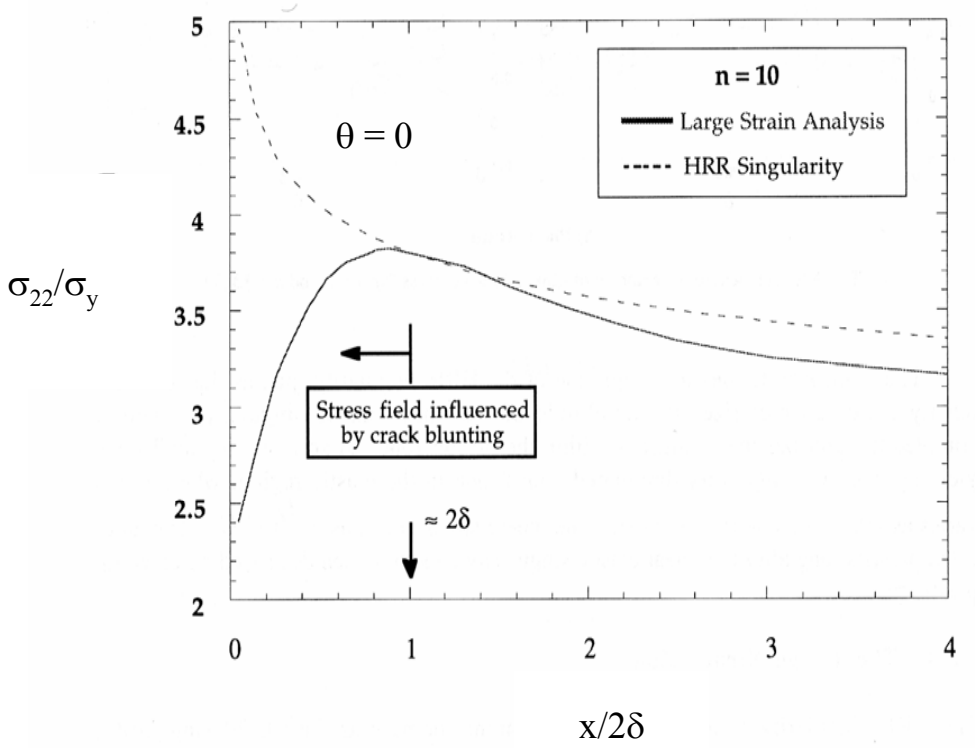

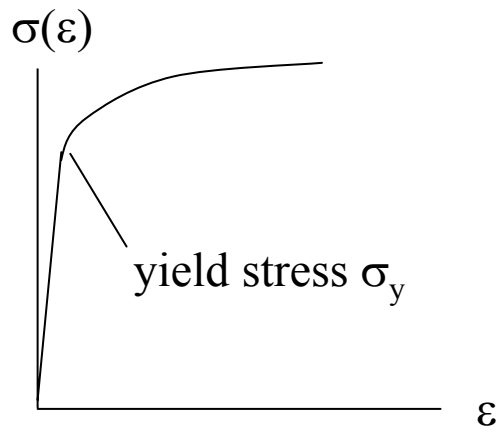

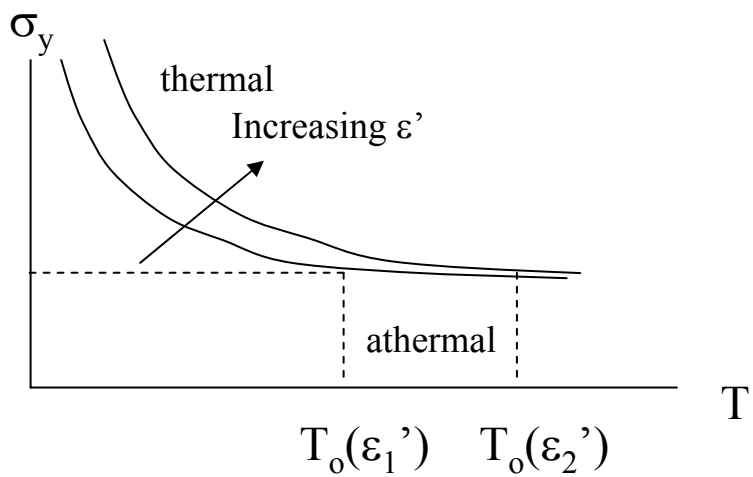

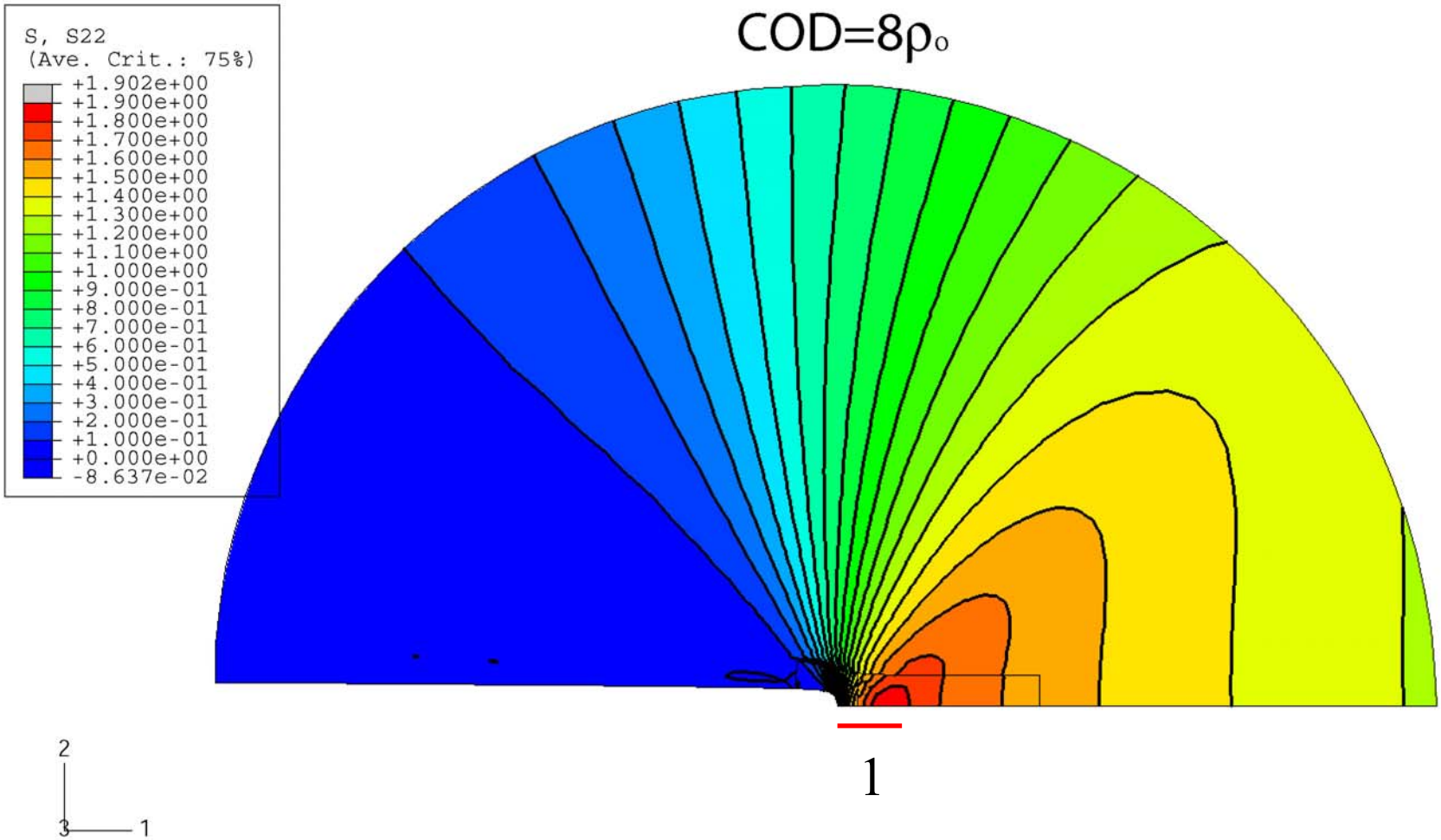
S, S22
(Ave. Crit.: 75%)
+1.902e+00
+1.900e+00
+1.800e+00
+1.700e+00
+1.600e+00
+1.500e+00
+1.400e+00
+1.300e+00
+1.200e+00
+1.100e+00
+1.000e+00
+9.000e-01
+8.000e-01
+7.000e-01
+6.000e-01
+5.000e-01
+4.000e-01
+3.000e-01
+2.000e-01
+1.000e-01
+0.000e+00
-8.637e-02
COD=8ρo
1
2
3
1

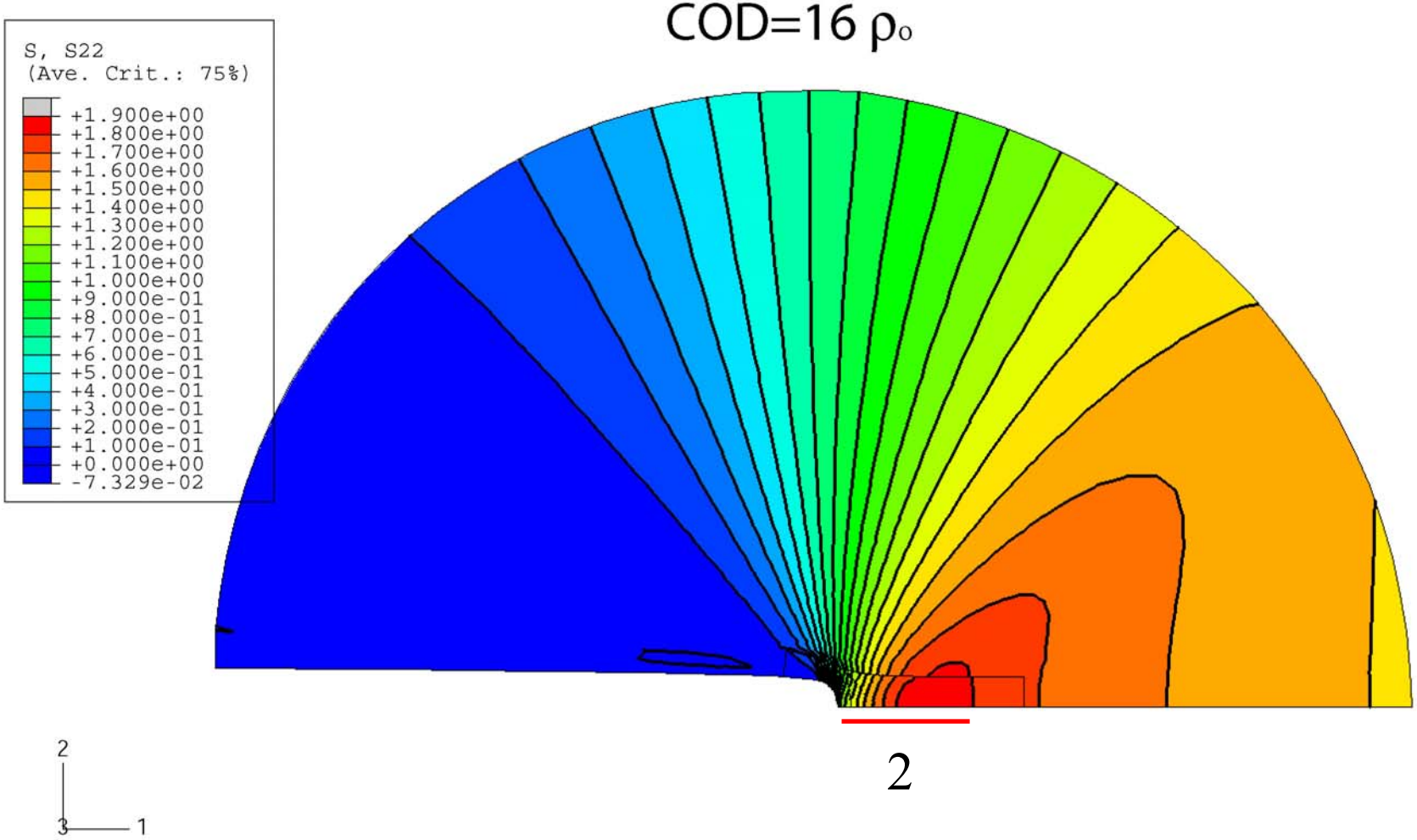
COD=16 ρo
S, S22
(Ave. Crit.: 75%)
+1.900e+00
+1.800e+00
+1.700e+00
+1.600e+00
+1.500e+00
+1.400e+00
+1.300e+00
+1.200e+00
+1.100e+00
+1.000e+00
+9.000e-01
+8.000e-01
+7.000e-01
+6.000e-01
+5.000e-01
+4.000e-01
+3.000e-01
+2.000e-01
+1.000e-01
+0.000e+00
-7.329e-02
2
3
1
2

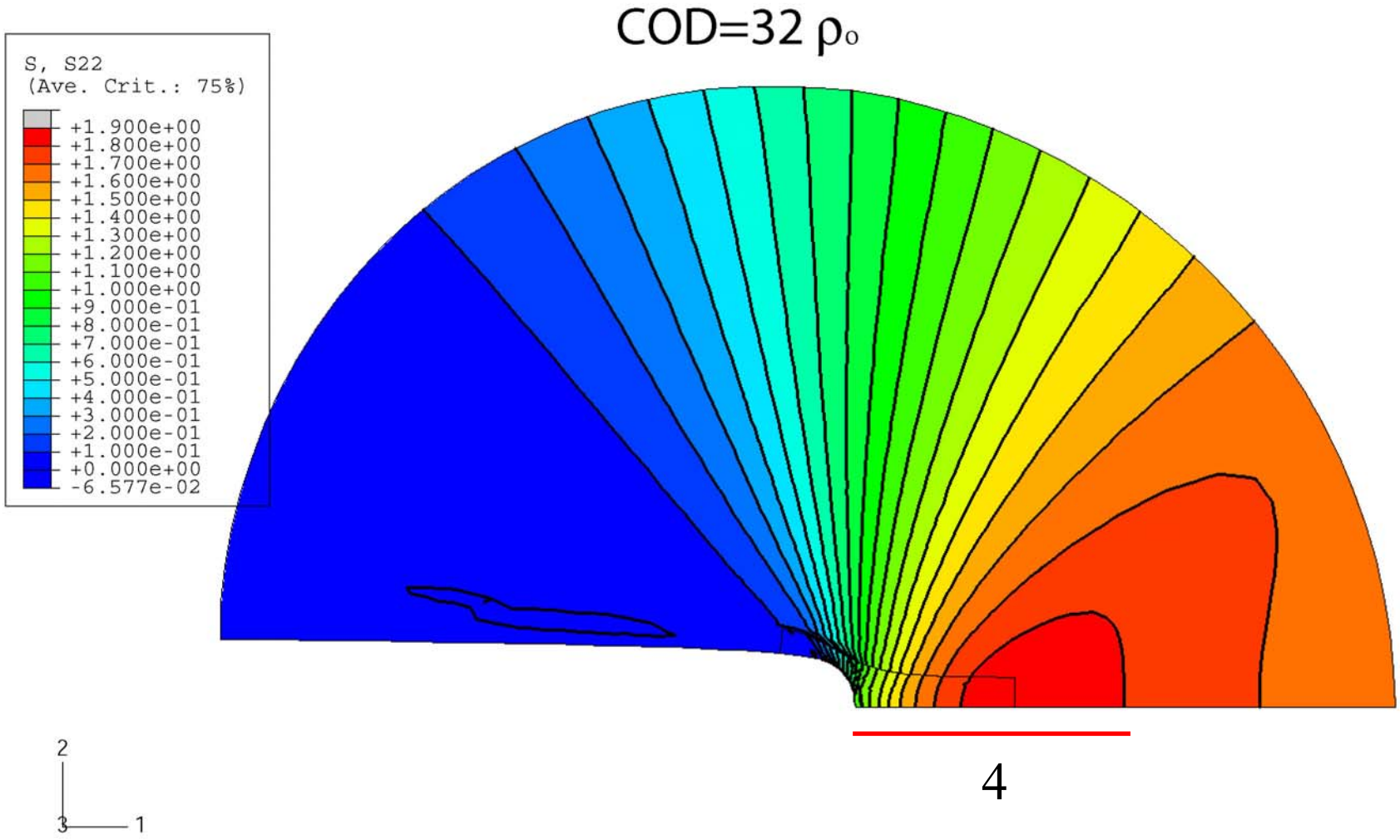
COD=32 ρo
S, S22
(Ave. Crit.: 75%)
+1.900e+00
+1.800e+00
+1.700e+00
+1.600e+00
+1.500e+00
+1.400e+00
+1.300e+00
+1.200e+00
+1.100e+00
+1.000e+00
+9.000e-01
+8.000e-01
+7.000e-01
+6.000e-01
+5.000e-01
+4.000e-01
+3.000e-01
+2.000e-01
+1.000e-01
+0.000e+00
-6.577e-02
4
2
3
1

Multiscale Fracture Processes

10 m

Macroscopic Scale

structure

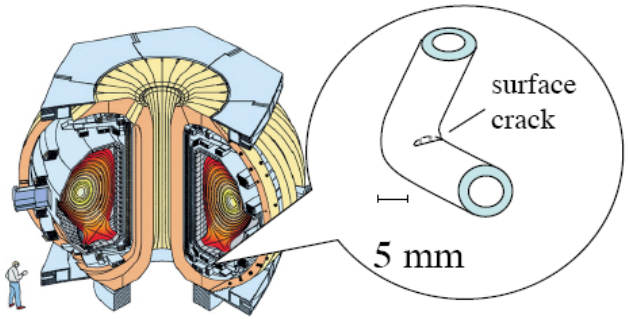

specimen

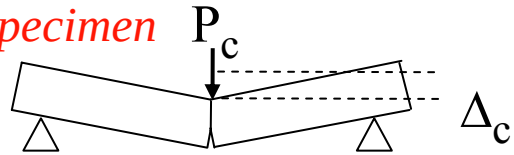

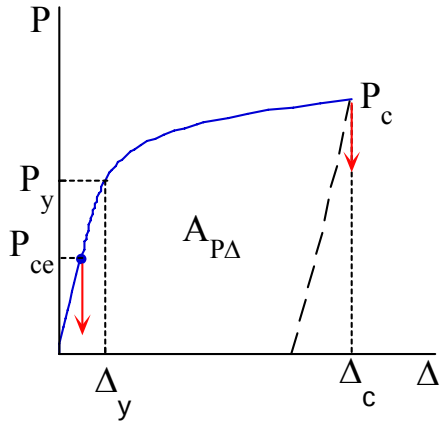

10^{-2}m

Critical structural fracture loads & displacements
controlled by $\sigma(\varepsilon)$, K_{Je}
FE models

Meso Scale

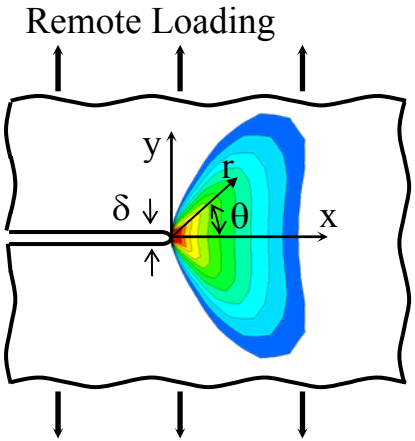

(a)

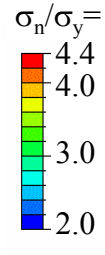

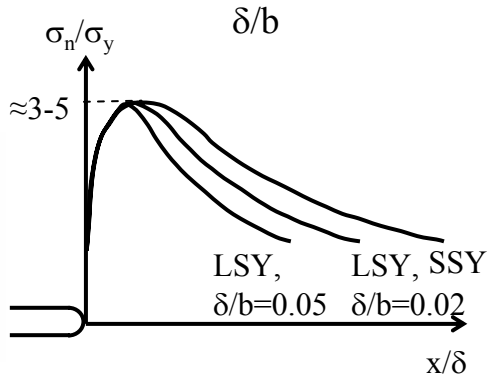

(b)

Crack tip stress & strain fields
controlled by $\sigma(\varepsilon)$, K_J & cracked-body size & geometry
FE models

10^{-5} m

Multiscale Cleavage Fracture Processes

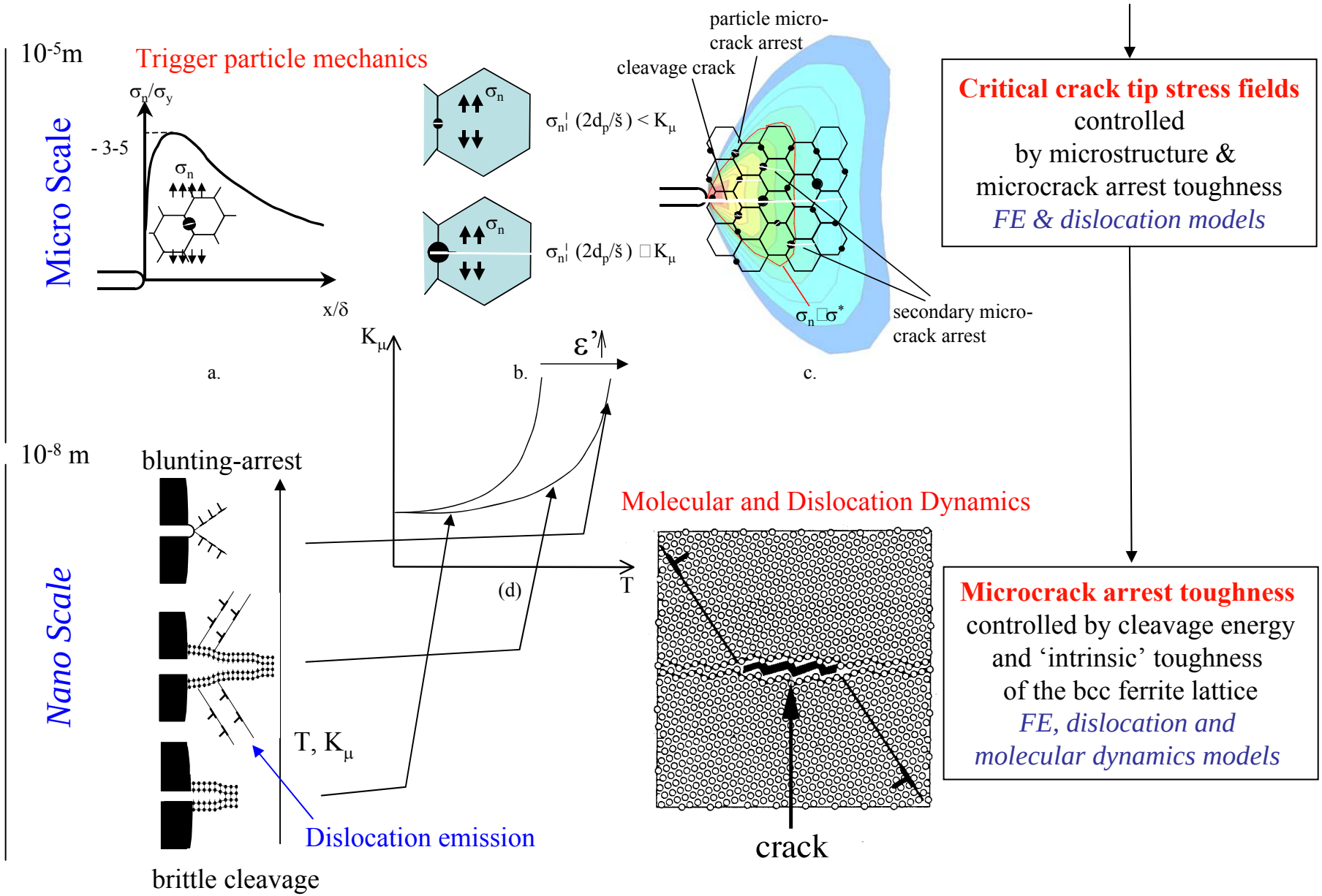

The SSY Master Curve - $K_{Jc}(T - T_o)$

- Microstructure => $\sigma(\varepsilon)$ + *local* fracture properties => $K_{Jc}(T)$
- Wide range $K_{Jc}(T)$ for various alloys and conditions
- But approximately universal $K_{Jc}(T)$ shape (Wallin)
- $K_{Jc}(T-T_o)$ collapses data - T_o usually taken at K_{Jc} =100 MPa$\sqrt{m}$
  - Universal shape?
  - If so - why?
  - Treatment of size effects?
  - Embrittlement - ΔT_o

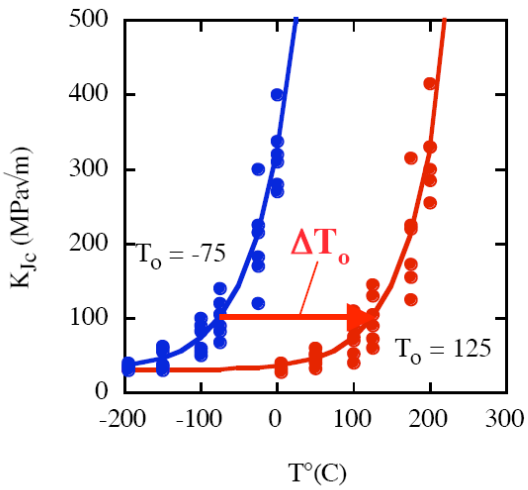

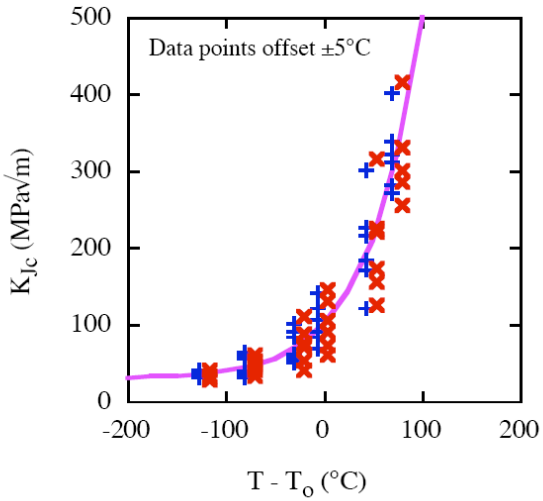

Micromechanical Models

- Critical stress ($\sigma_{22} = \sigma^*$) - critical distance (λ^*) (RKR)
- Critical stress ($\sigma_{22} = \sigma^*$) - critical area (A^*)/volume (V^*)
- Statistical (Weibull) $P_f = 1 - \exp([-\sigma_w/\sigma_o]^m) \Rightarrow \sigma_w =$ volume averaged power (m) weighted $(\sigma_{22}^m)^{1/m}$ stress
- A^*/V^*, σ^*, m and $\sigma_o \Rightarrow$ *local fracture properties* controlled by microstructure and ferrite lattice properties

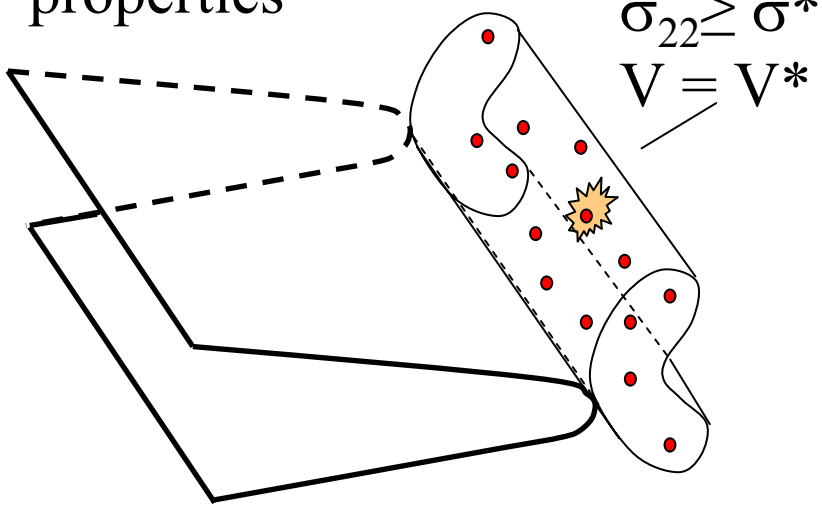

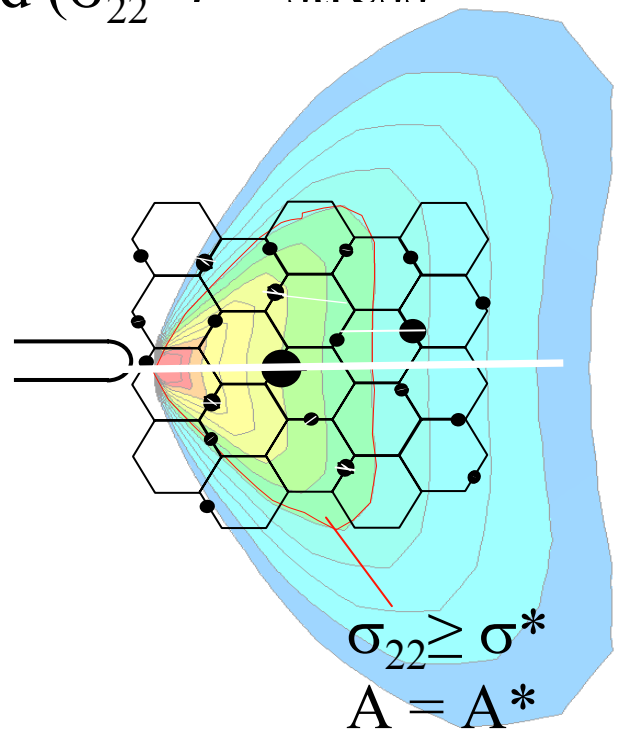

Universal SSY MC Shape?

- Why universal shape for wide range of microstructures & T_o?
- $A=A^*$, $\sigma_{22}=\sigma^* \neq f(T)$ => SSY master curve $K_{Jc}(T-T_o)$ low T_o
- $K_{Jc}(T)$ shape due to $\sigma_y(T)$
- Magnitude $\sigma_y(T)$ sensitive but shape insensitive to microstructure

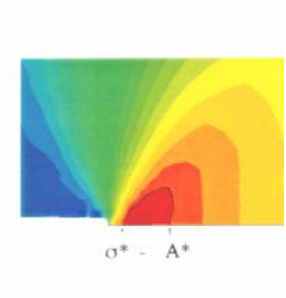

Cracked body geometry or SSY boundary layer + $\sigma(\varepsilon,T)$ => FE => $A(\sigma_{22}/\sigma_y, K_J)$

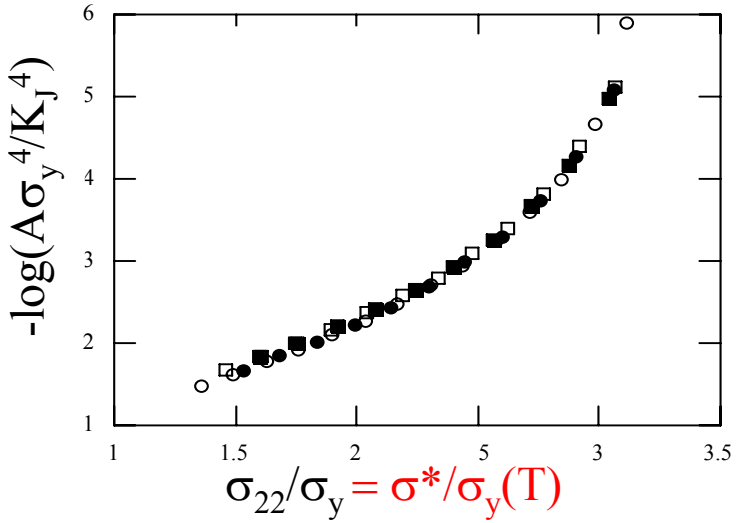

+ σ*, A*

Example
T_o = -45°C
σ* = 1900 MPa
A* = 10^{-8} m²

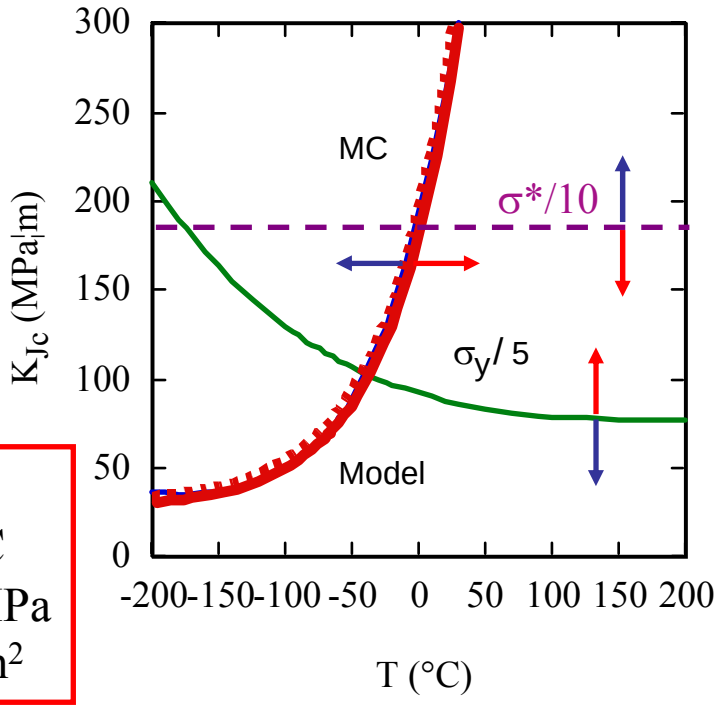

Embrittlement - ΔT_o

- Embrittlement - $\Delta\sigma_y > 0$ (or $\Delta\sigma^* < 0$) => ΔT_o
- Large ΔT_o up to > 300°C observed for large $\Delta\sigma_y$
- If $\sigma^* \neq f(T)$ => $K_{Jc}(T) \neq$ master curve shape for $T_o > 0°C$
- Universal shape requires $\sigma^*(T)$
- But σ^* depends on microstructure?
- Intrinsic property => universal $K_{Jc}(T-T_o)$?
- Intrinsic lattice micro-arrest toughness K_μ

Irradiation hardening by nanoprecipitates

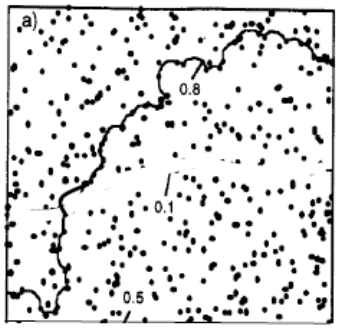

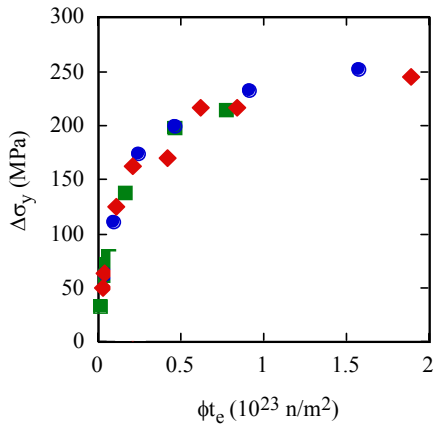

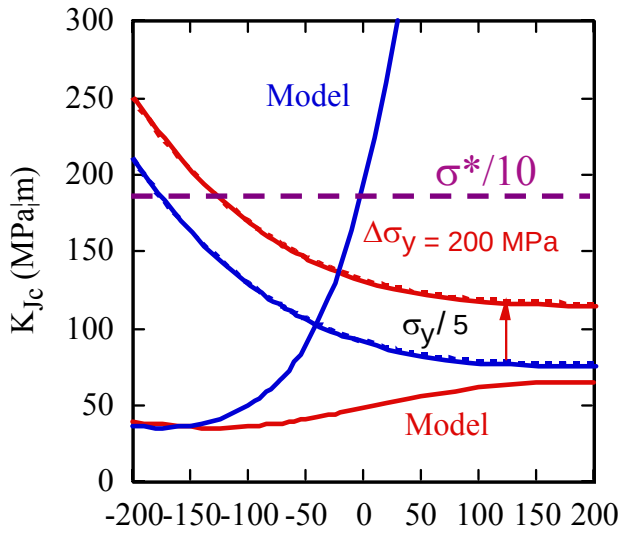

ΔT_o- $\Delta\sigma_y$ Correlation - RPV Steels

- Excellent agreement with previous data compilation by Sokolov - but extended to much higher levels of hardening and embrittlement – $\Delta T_o/\Delta\sigma_y$ - 0.69 (previous) vs 0.71 (new) ° C/MPa

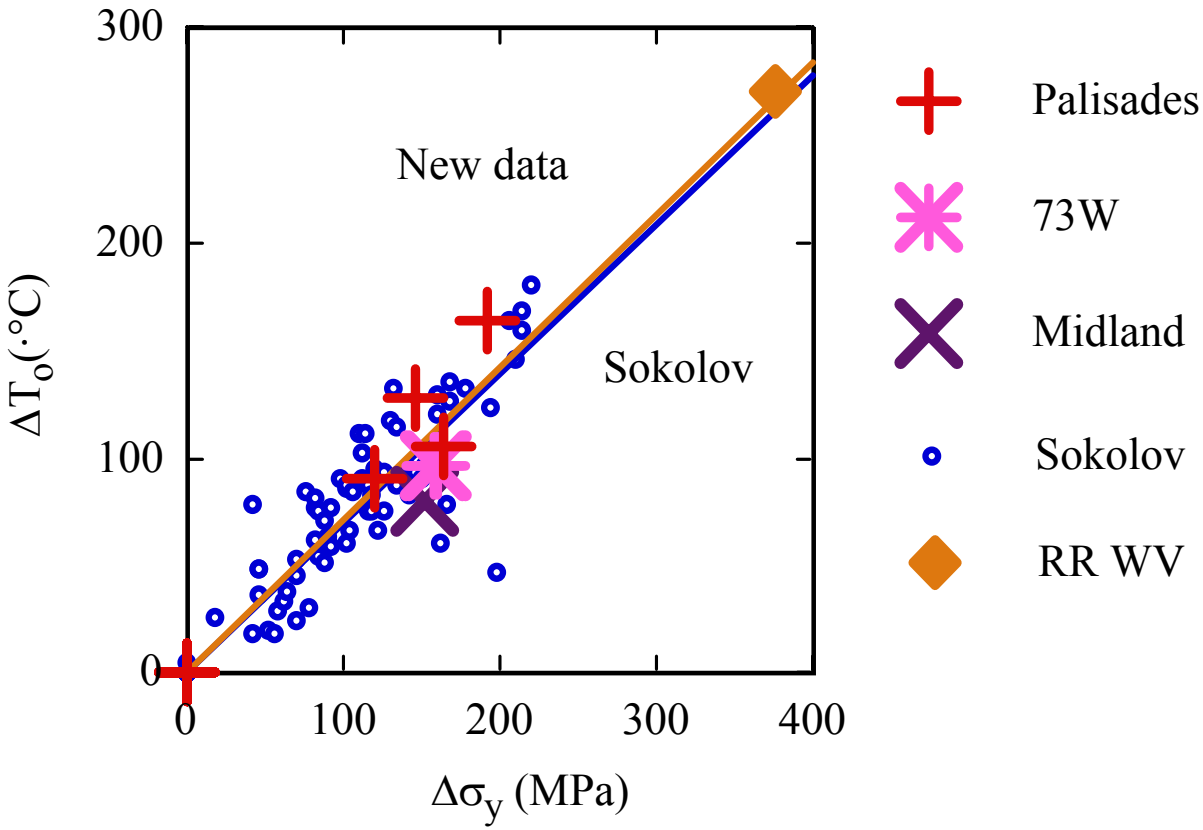

$\sigma^*(T)$ and $K_\mu(T)$

$$\sigma^*(T) = C_g K_\mu(T)\sqrt{d_p}$$

Broken trigger particle

d_p

new surface energy

$K_\mu \approx [2E(2\gamma + w_p(T)]^{1/2}$

elastic modulus

plastic work

σ_y

$\sigma^*/5$

σ_y or σ^* (MPa)

T (°C)

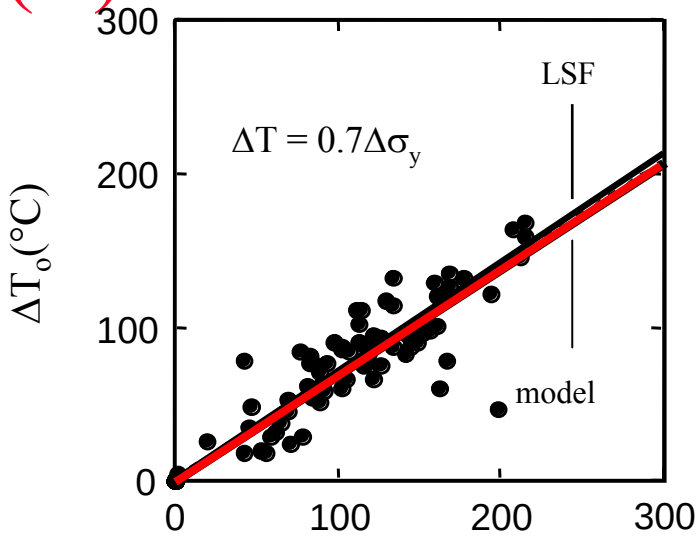

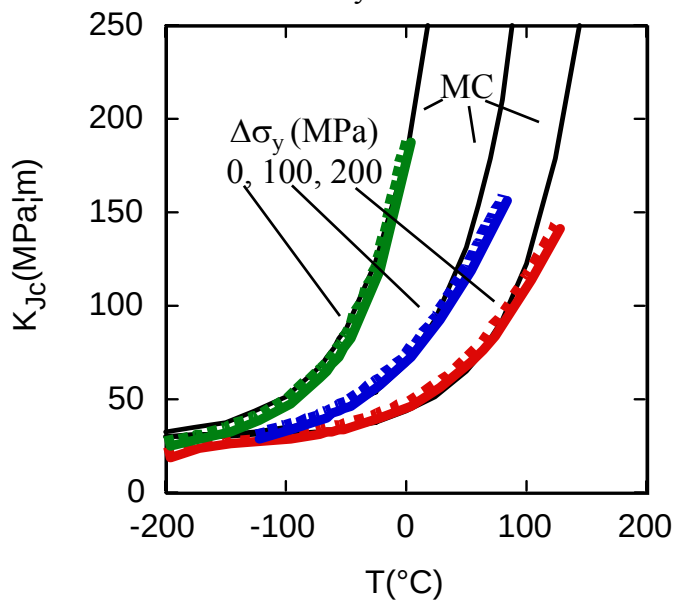

σ*(T) Controlled by Arrest $K_\mu(T)$

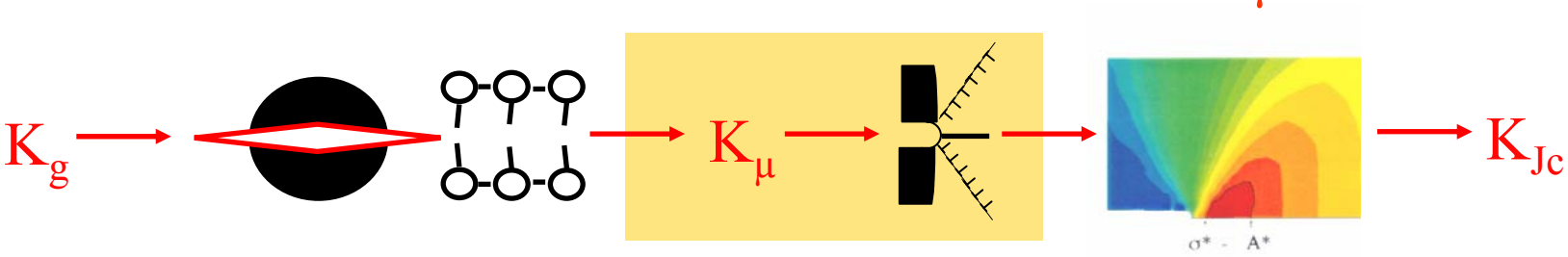

σ*(T) is controlled by the temperature dependence of $K_\mu(T)$

$$\sigma^*(T) = \frac{CK_\mu(T)}{\sqrt{d}}$$

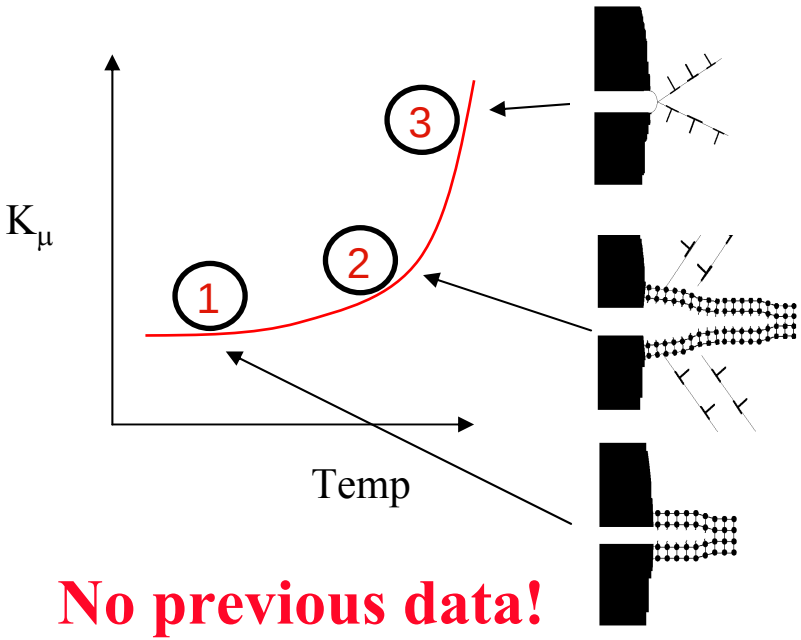

No previous data!

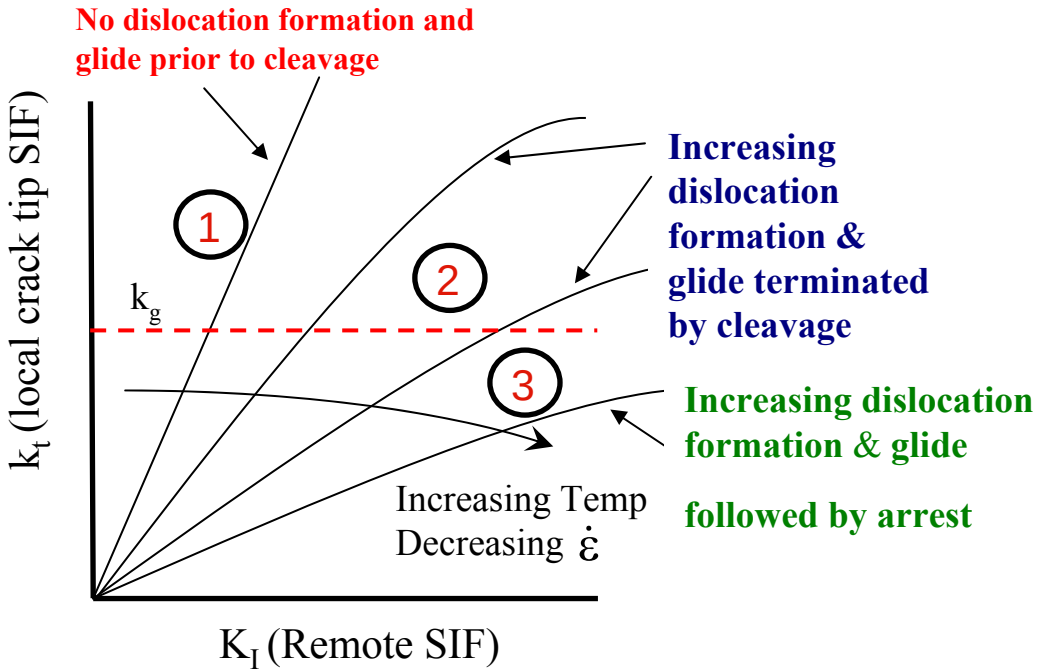

Composite Specimen Single Crystal Tests

- Finite element model of K(a/W) confirmed by TiAl calibration

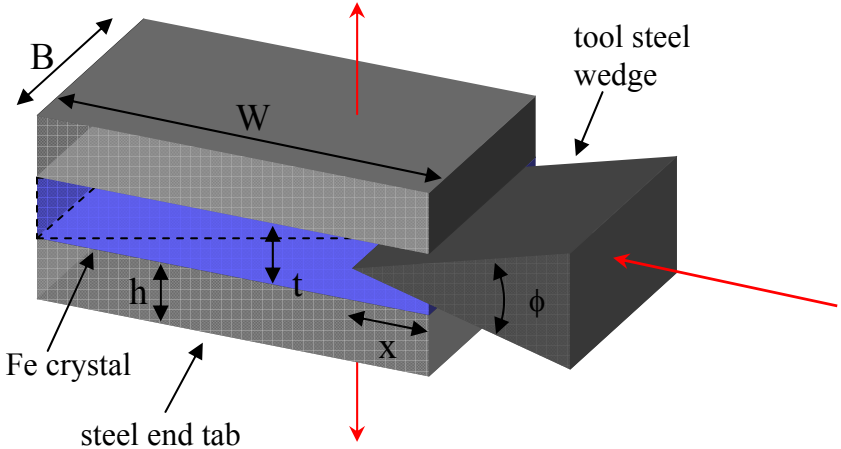

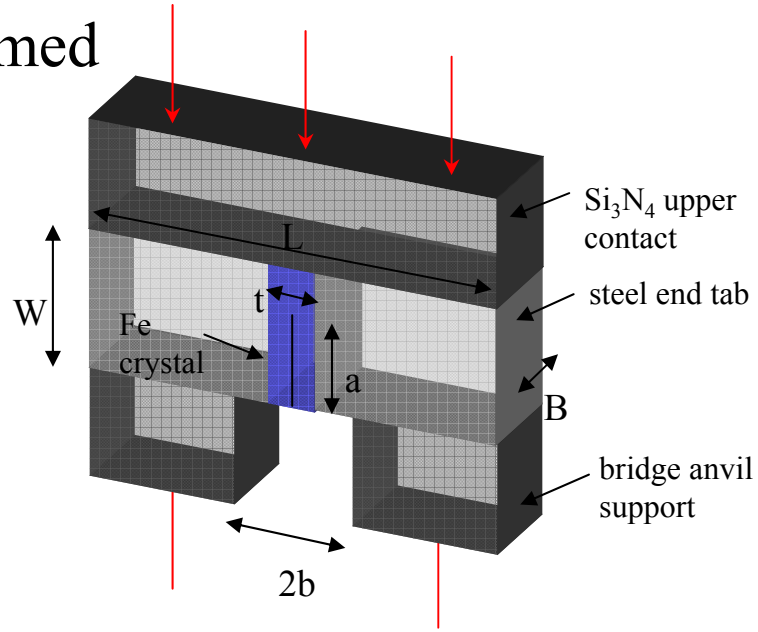

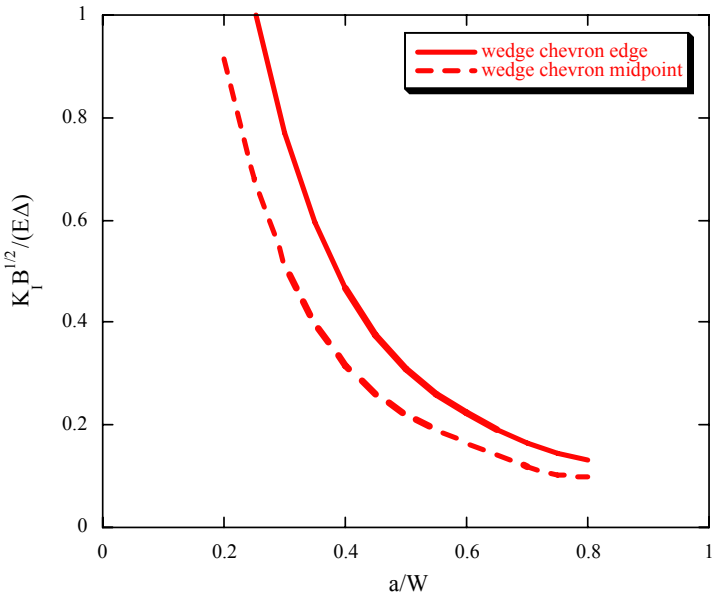

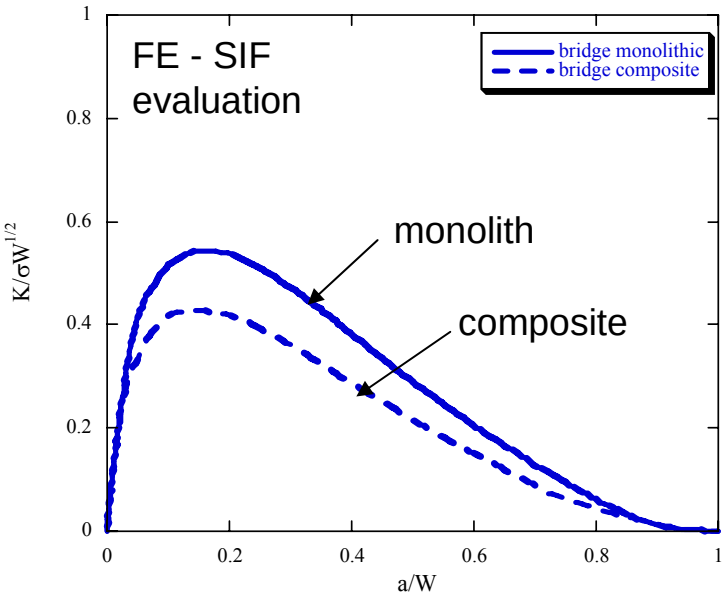

$K_a(T)$

- Two low toughness cleavage orientations
- Two test methods
- For (100) mean $K_a(T)$ increase from ≈ 3.5 MPam$^{1/2}$ @ -196° C to ≈ 9 MPa-m$^{1/2}$ @ 0° C similar for both orientations and methods
- At lowest T-minimum K_a values ≈ 2 MPa-m$^{1/2}$

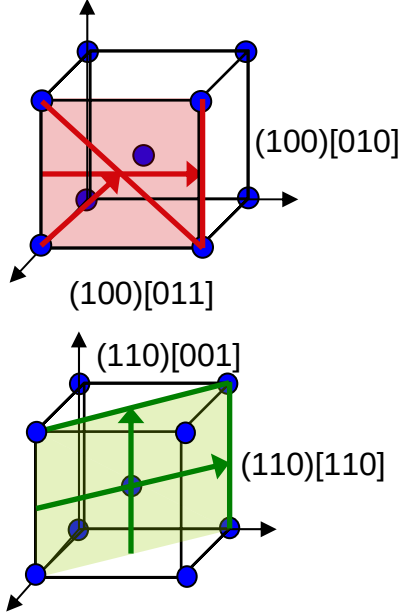

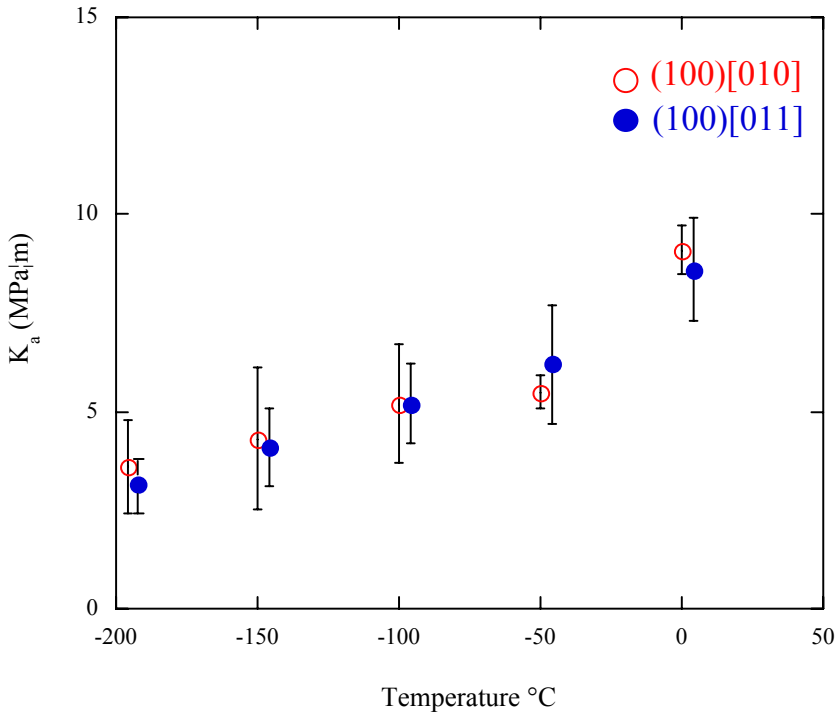

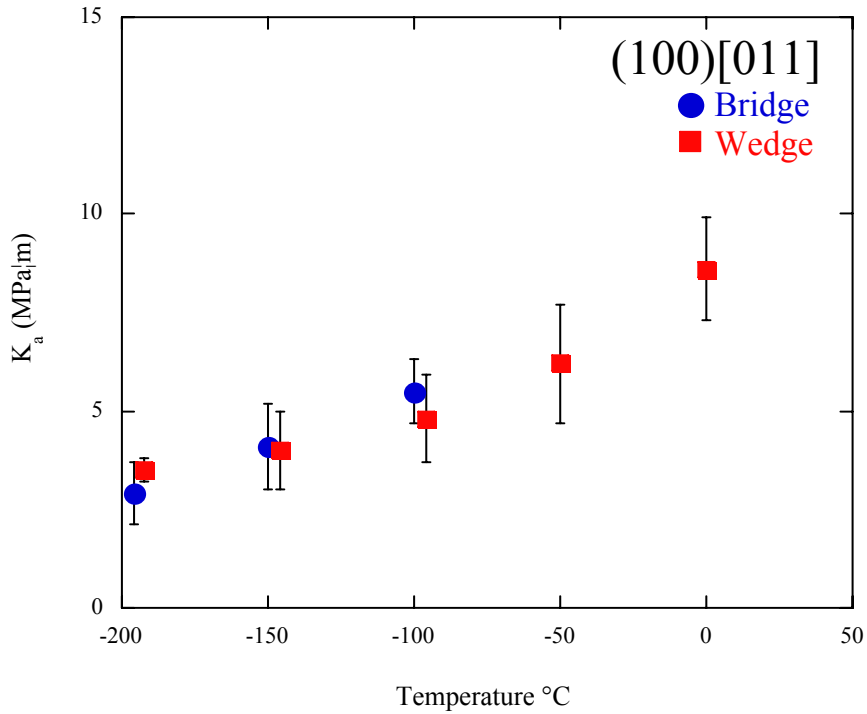

Initiation $K_{Ic/d}(T)$

- Bridge specimens left with long sharp precrack
- Test in 4-point bending
- Explore $K_I \sim 0.1\text{-}2\times10^4$ MPa-$m^{1/2}$/s @ -196° C to 50° C

$\dot{K}$ (MPa $\sqrt{m}$ / sec)

- ~ 0.1
- ~1
- ~10^3
- ~10^4

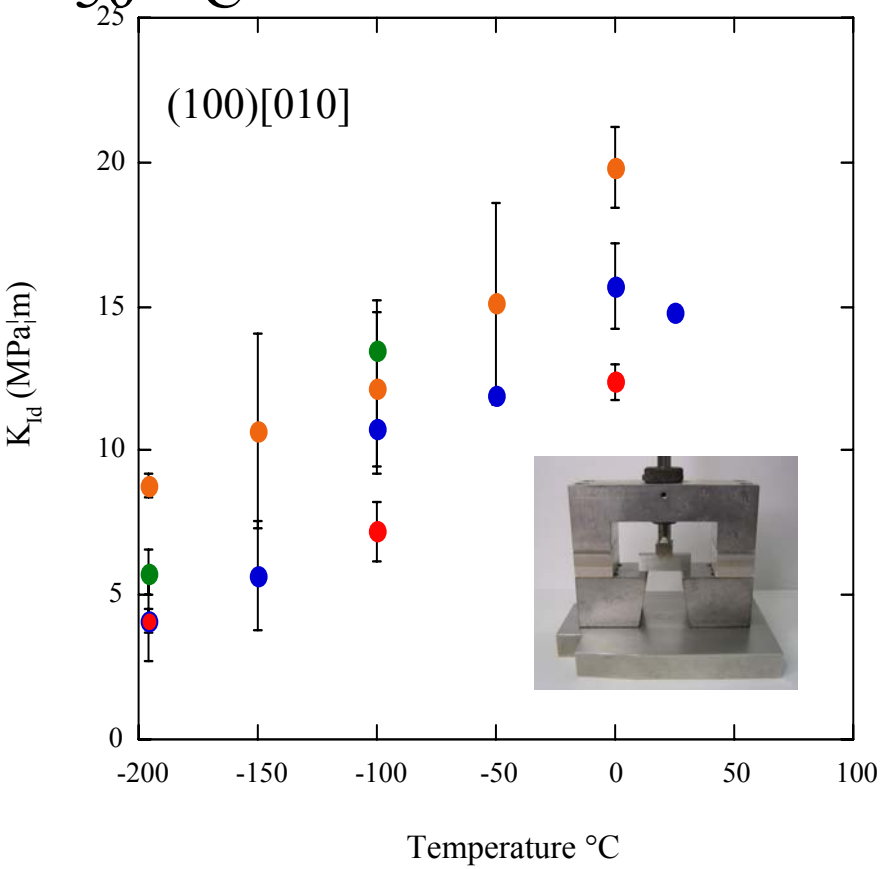

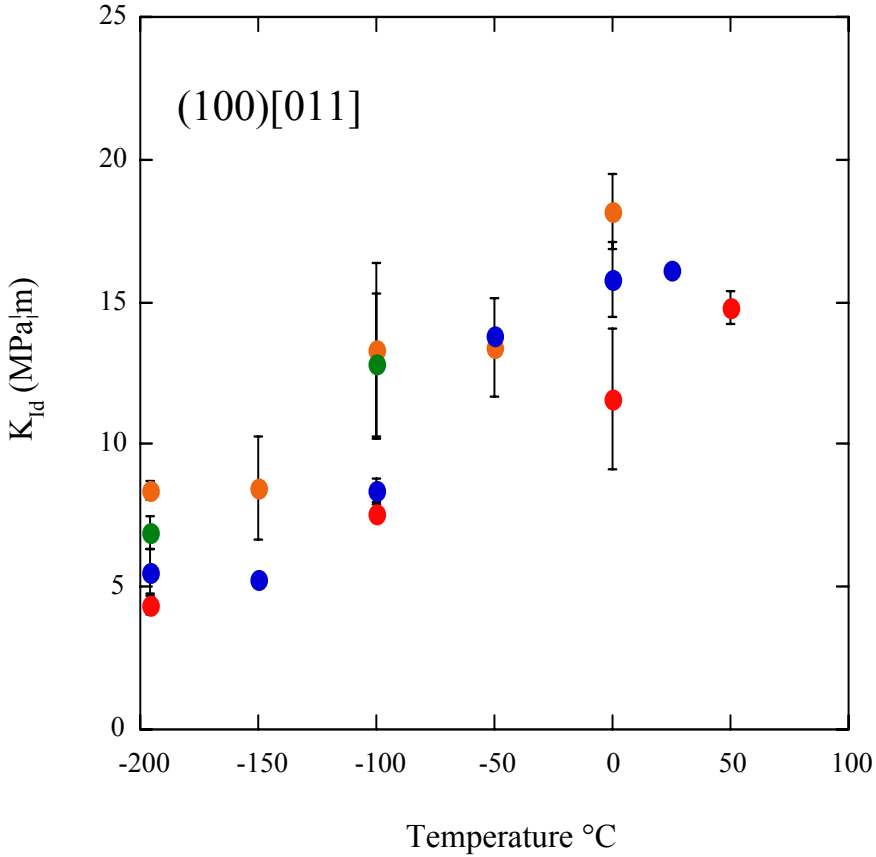

Activation Energy - U*

- K' and T dependence -> thermally activated process - U*(σ)
- U* increases with decreasing σ_y & increasing T (and K_a)
- Dynamics very similar to yield dynamics

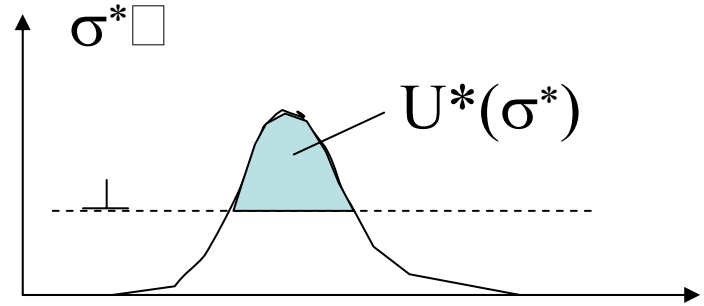

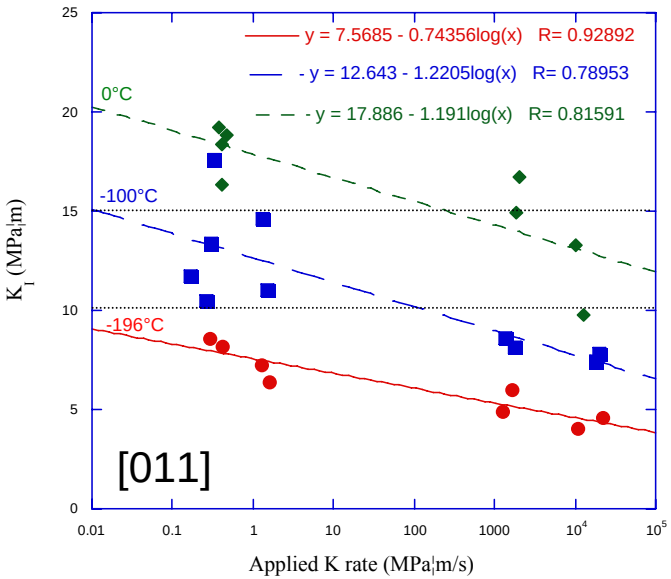

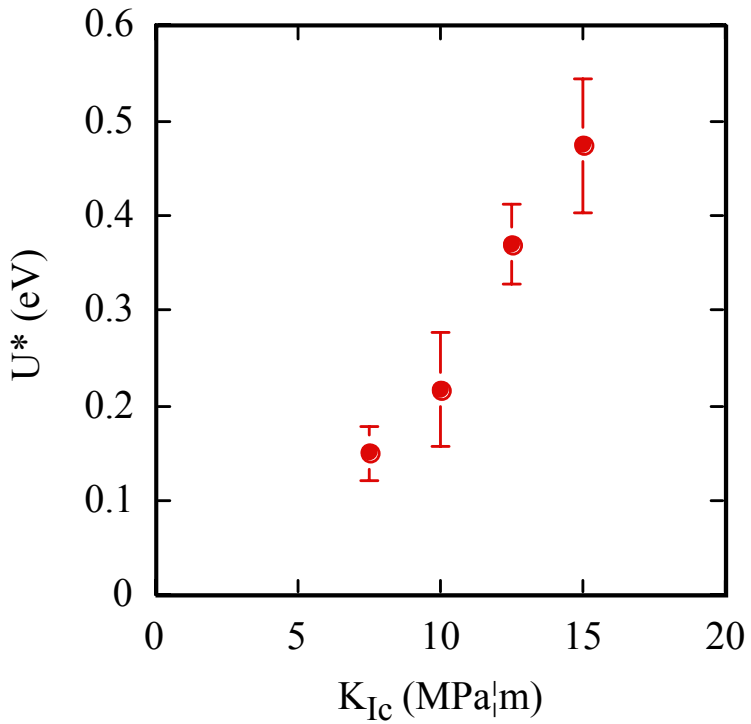

$\sigma_{yth}(T, \varepsilon')$

- $\sigma_y = \sigma_{yth}(T, \varepsilon') + \sigma_{yat}$
- Dislocation dynamics $\sigma_{yth}(T, \varepsilon')$ -> controlled by stress (temperature) dependent activation energy - $U^*(\sigma)$
- $U^*_{max} \approx \alpha k T_o$ where $\sigma_{yth} = 0$ at $T > T_o(\varepsilon')$
- σ_{yth} data for various ε' collapses on a strain rate compensated T' scale for selected reference ε_r': $T' = T[1 - (1/\alpha)\ln(\varepsilon'/\varepsilon_r')]$

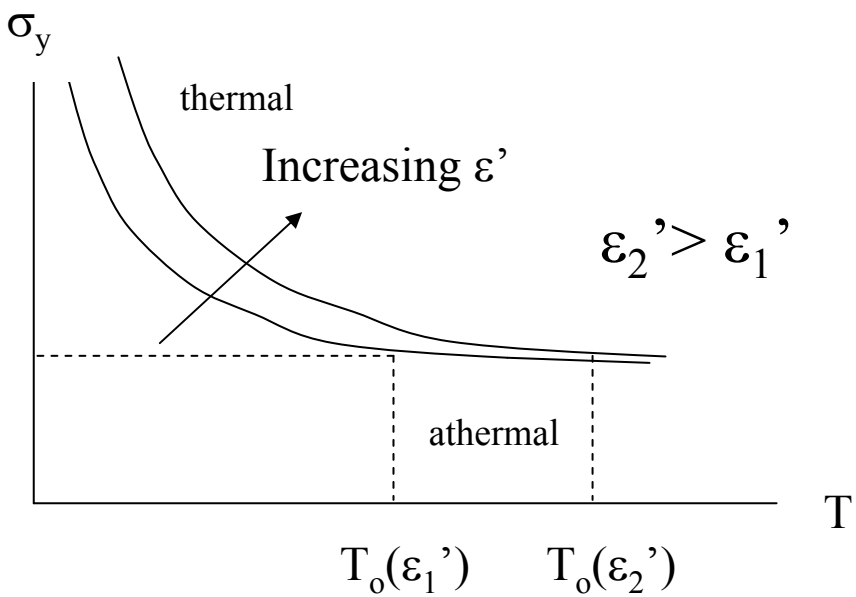

Double Kink Nucleation

- σ_{yth} primarily depends on double kink nucleation on screw dislocations
- Double kink nucleation also governs U^*_{max} and the shape of the $\sigma_{th}(T')$ curve
- Total of 19 alloys

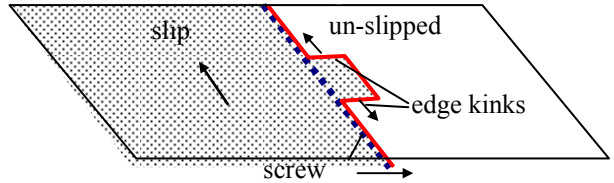

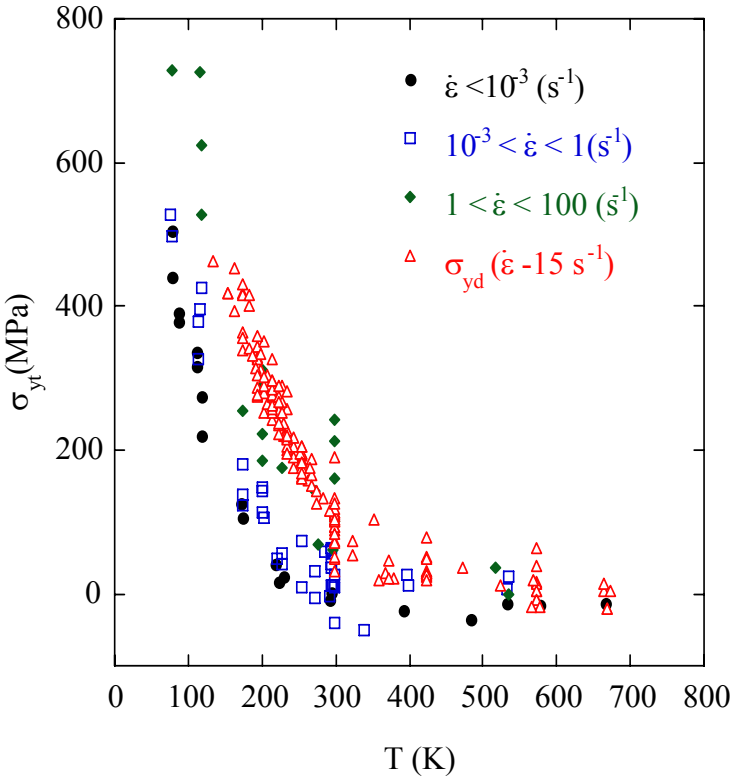

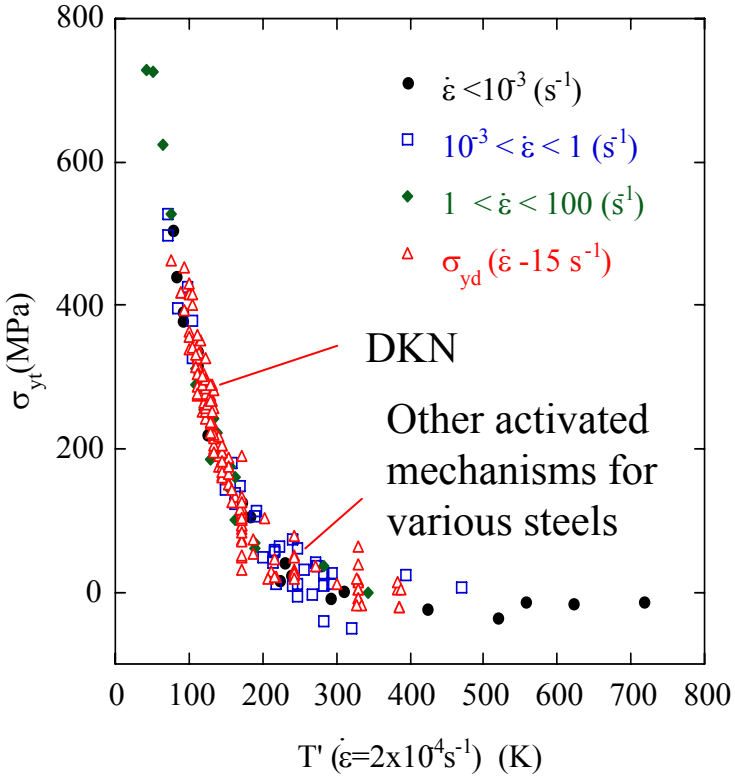

$K_{Ic/d}$-K_a Master Curve

- Adjusted rate dependent data will also yield an estimate of U^*_{max} at reference K' = 10^4 MPa-$m^{1/2}$/s
- Collapses all $K_{Ic/d}(T)$ & $K_a(T)$ into a single trend curve

From estimates of Charpy impact rates:

For $\dot{K} = 10^4$ $\dot{\varepsilon} = 20/s$

For $\dot{K} = 10^3$ $\dot{\varepsilon} = 2/s$

For $\dot{K} = 10^0$ $\dot{\varepsilon} = 2x10^{-3}/s$

$\dot{\varepsilon}$ arrest = 5000/s

$T_o = 536°$ K, $U^*_{max} = 0.69$ eV

Adjust toughness to 10^4/s,

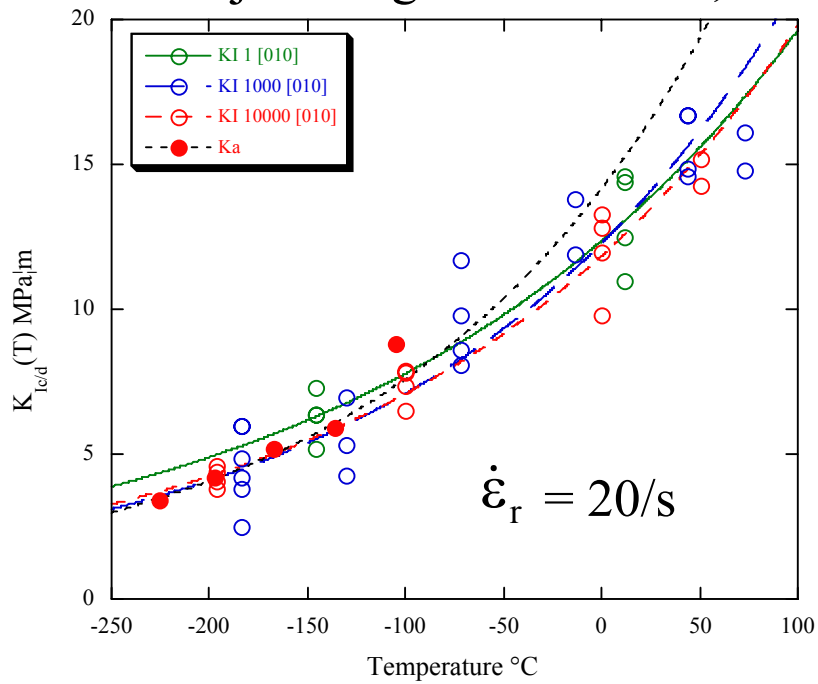

≈ consistent with double kink nucleation mechanism

Deformation-Cleavage Dynamics

Observed that yield dynamics fracture dynamics are the same

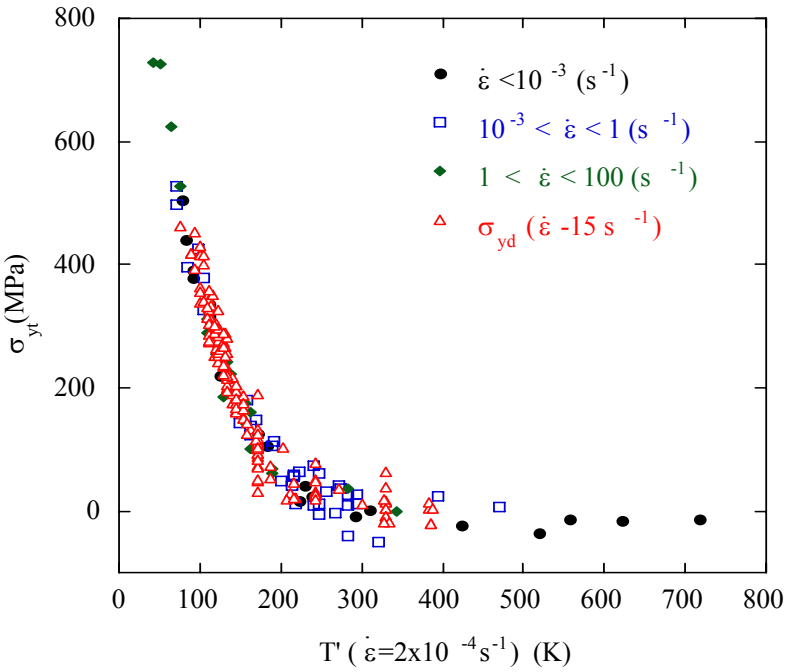

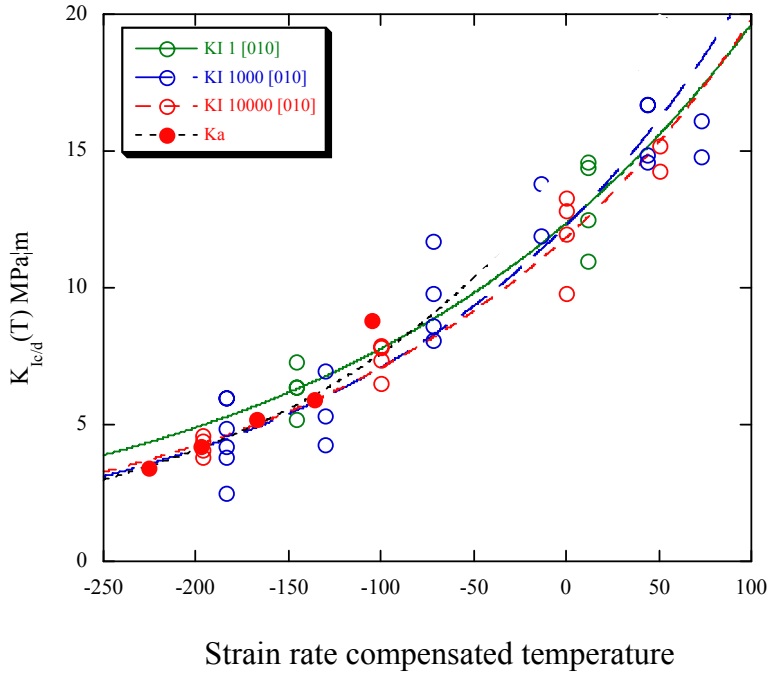

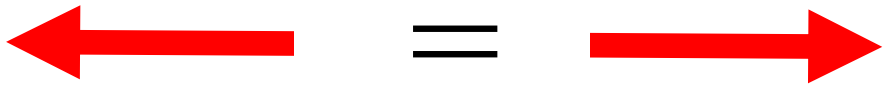

[011] Cross Section Slip Traces

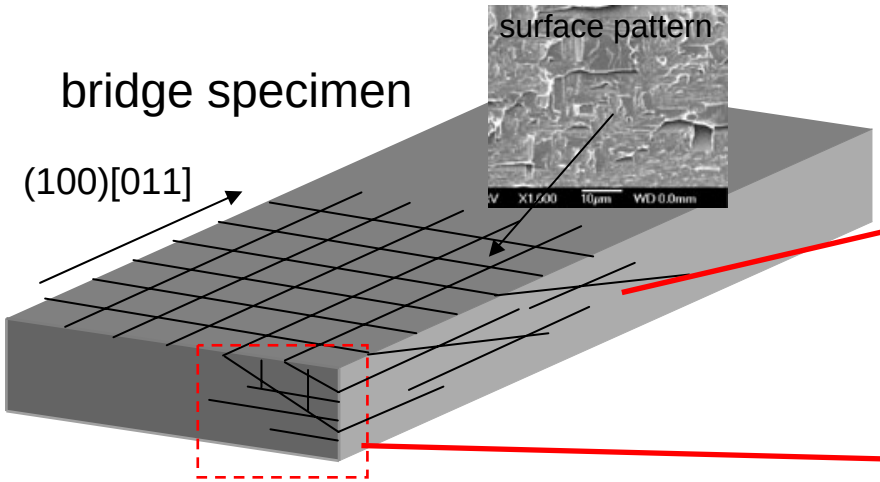

Observed x-section slip trace patterns

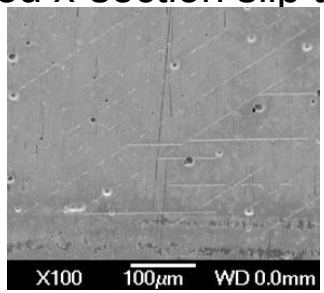

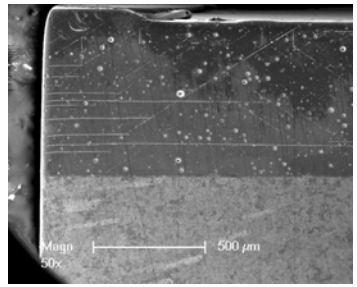

Additional vertical crack x-section slip traces attributed {110} systems

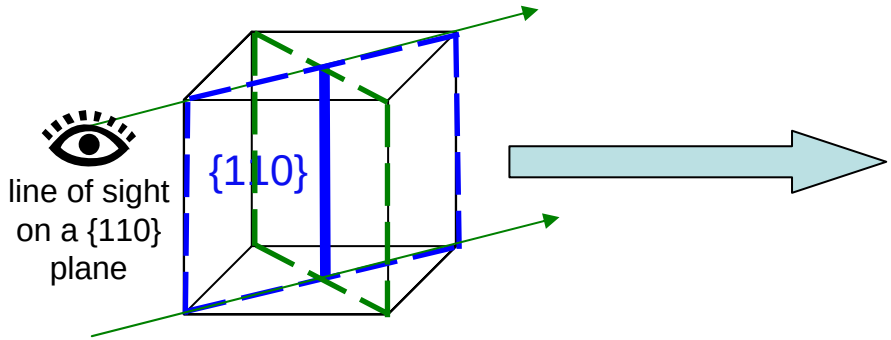

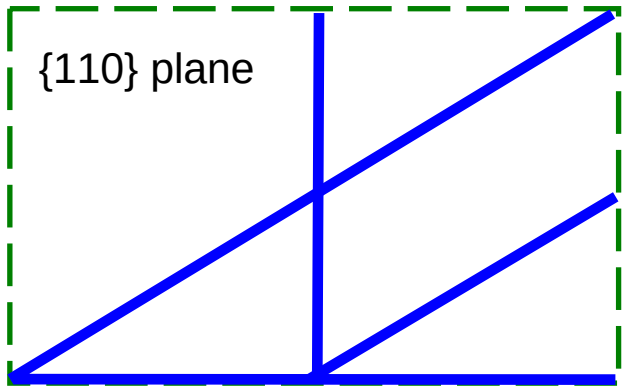

Slip traces confirm both {110}<111> and {211}<111> systems active

Does *Total* $\sigma_y(T)$ Mediate $K_a(T)$?

- $K_a(T)\sigma_y(T) \approx C_{sc}$
- Fit $\sigma_y^{-1}(T)$ to $K_a(T)$ data assuming arrest $\varepsilon' = 5x10^3/s$ for single crystal with $\sigma_{ath} = 100$ MPa
- $K_a(T)$ for $\sigma_{ath} \geq 100$ is also $C_{sc}/\sigma_y(T)$
- Reasonable fits Fe-3Si (Argon)

& W (Gumbsch)

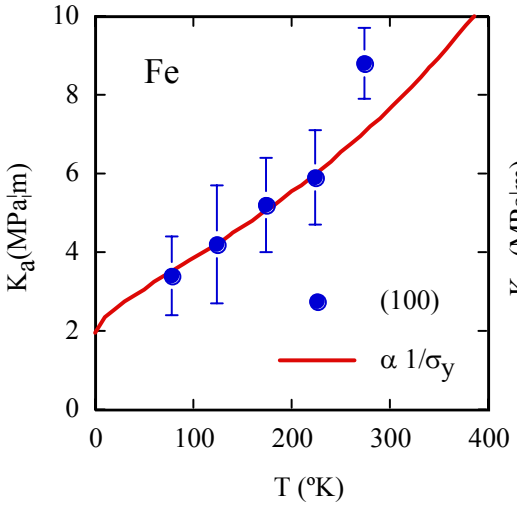

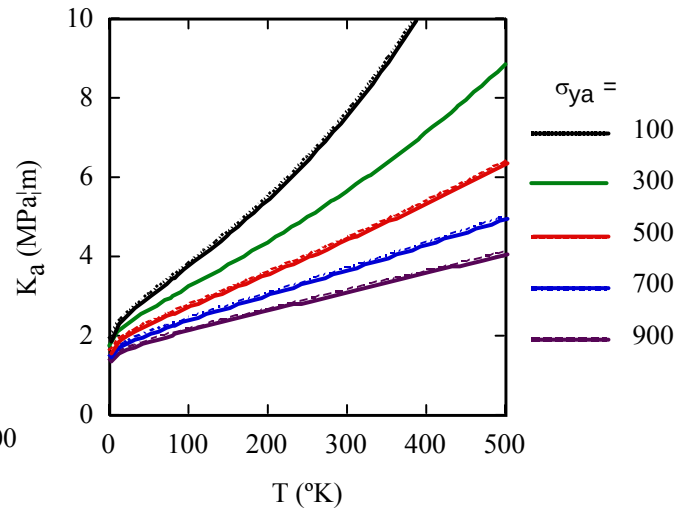

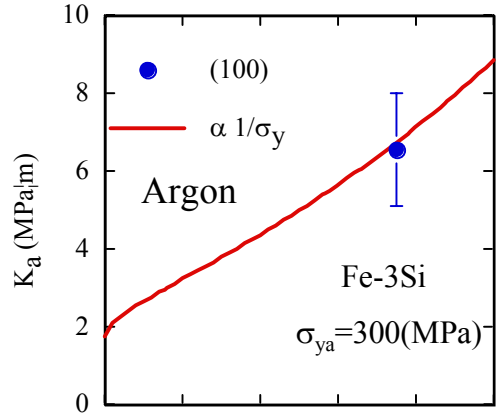

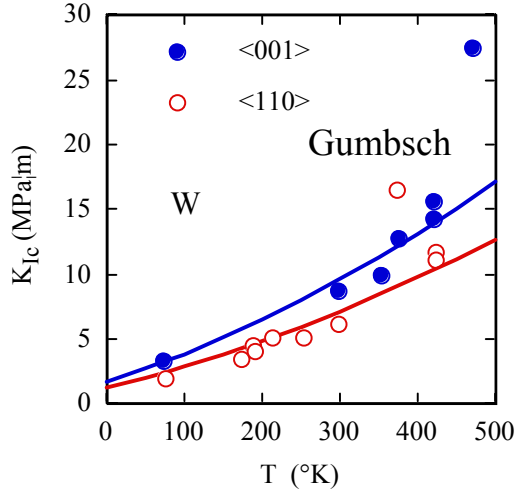

Master Curve Model

- $K_a(T) = C_{sc}/\sigma_y(T,\varepsilon')$ for $K_a(T) > K_{amin}$
- $K_{amin} = 3.25$ MPa-$m^{1/2}$ for polycrystalline Fe alloys
- K_{Jc} - $\sigma^*(T)$ [from $K_\mu = K_a(T)$], A* model
- $K_{Jc}(T)$ too steep at low T_o and $\Delta T_o/\Delta\sigma_y$ increases with $\Delta\sigma_y$
- Oversimplified/incomplete - T effect on strain hardening….?
- "Better" results for previous empirical K_μ curve

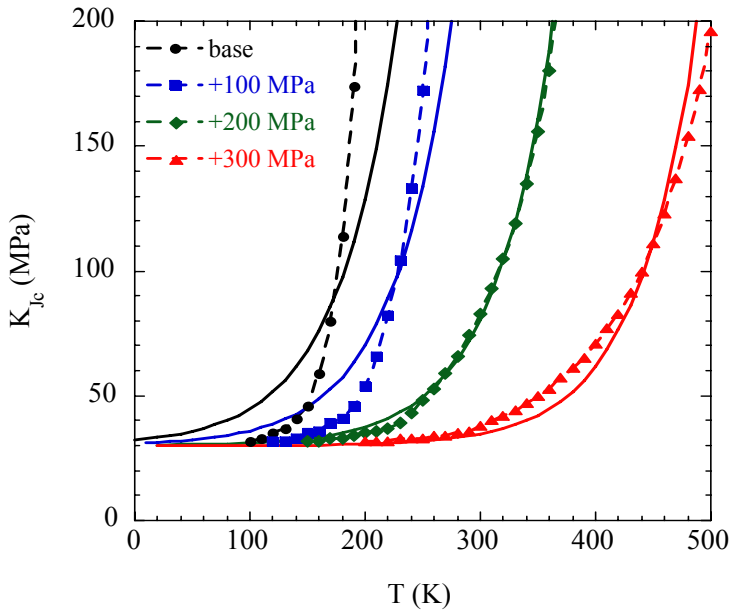

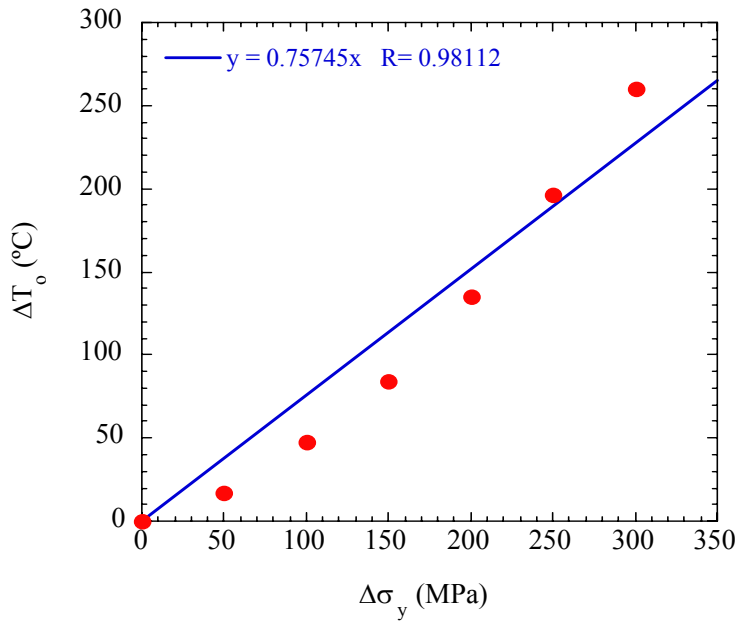

Size Effects on K_{Jm}

- Statistical -- weakest link statistics

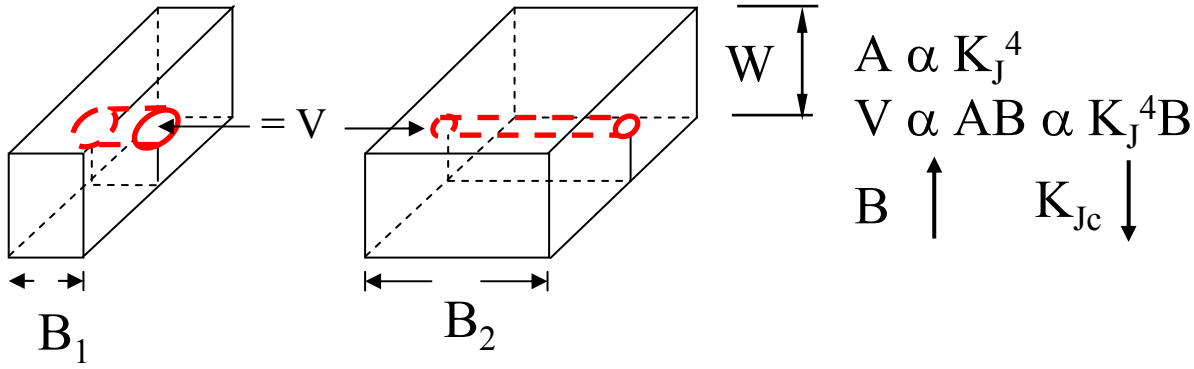

- In-plane constraint Loss -- SSY size deformation limits

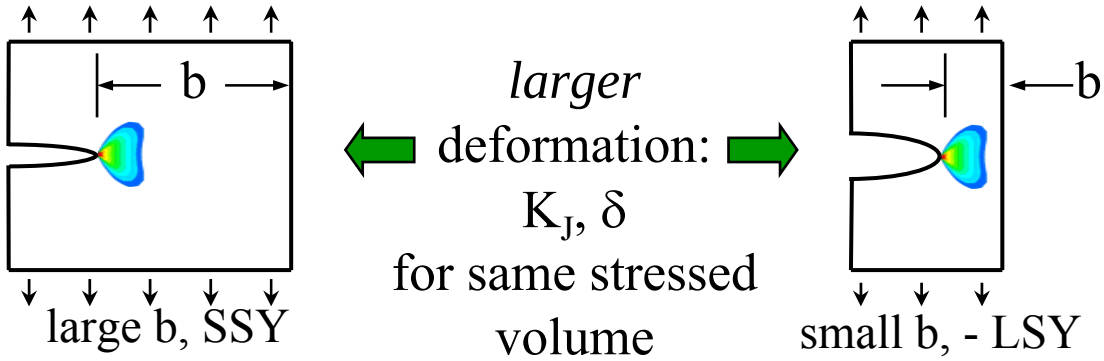

Deviations From SSY

- SSY crack tip dominance not norm - short, shallow cracks, ..
- SSY deformation limit $\delta_c < \approx$ (a, b, B)/100
- If not => lower σ_{22} - lose tri-axial constraint => size-geometry effects => *measured $K_{Jm} > K_{Jc}$ (SSY)*
- Use *local crack tip process zone* micromechanical model

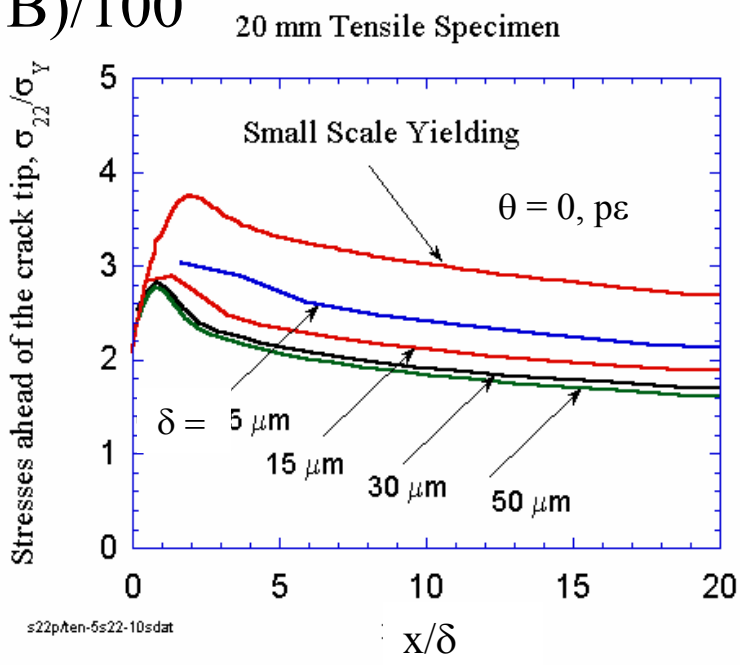

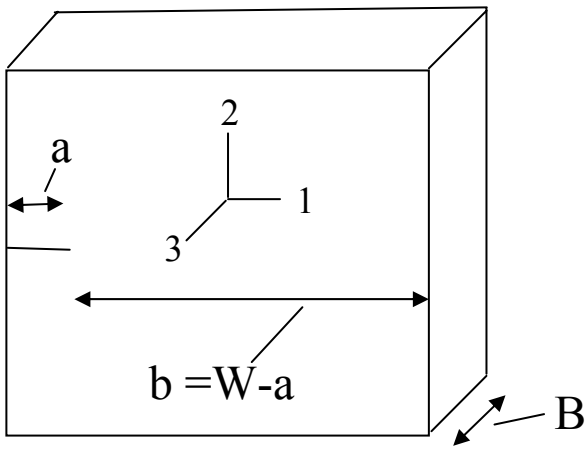

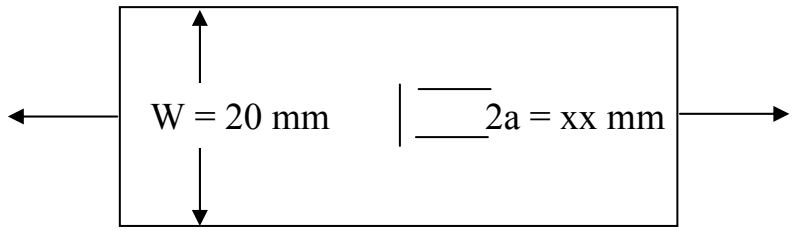

Statistical Size Effects

- Large intrinsic scatter in cleavage K_{Jc}
- Cleavage initiation => weakest link in *brittle trigger particle* distribution (P_f)
- K_{Jm} => critical stressed volume $V(\sigma_{22})$
- SSY: $V(\sigma_{22}) = C(\sigma_{22})BK_J^4$ =>

$$\mathbf{K_{Jm} \approx \alpha\, B^{-1/4}}$$

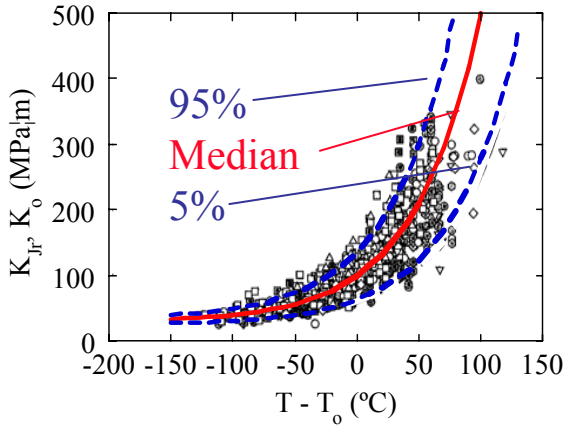

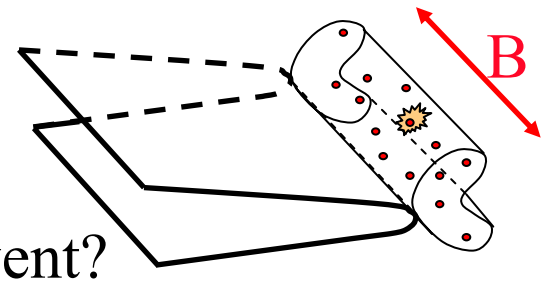

- Modified scaling - generally not a single event?
  - $K_{min} > 0$ at P_f -> 0
  - Upper and lower $B^{1/4}$ scaling limits?
  - Sympathetic versus single events
  - Damage accumulation-critical point instability

->

Size and Geometry Effects

- Use models to understand-treat size effects:

  K_{Jm} (coupon test) => K_{Jc} (SSY) => $K_{Jr}(B_r)$ => P-Δ (structure)

- Assess individual-combined constraint loss-statistical effects
- No previous 'single variable' database - predominant self-similar specimens => b α B
- H. Rathbun - first single-variable experiment designed to *decouple* sources size effects B = 8-254 and b = 3-25mm
  - seek large (≈ 2x) effects
  - multiple tests a/W ≈ 0.5
  - same steel* & test conditions
  - comprehensive ancillary database
  - model based analysis

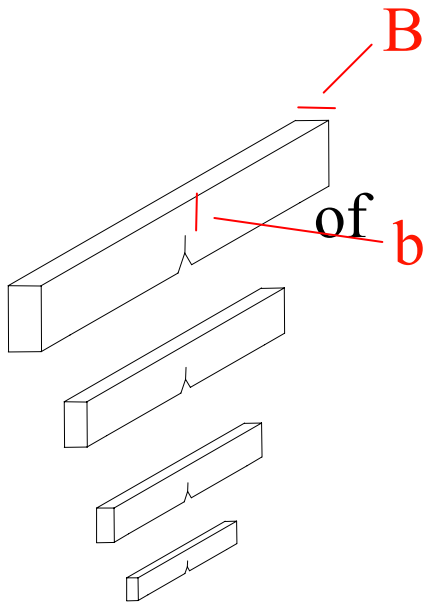

*from unused Shoreham vessel plate

Test Matrix

B = 8 to 254 mm and W = 3 to 25 mm

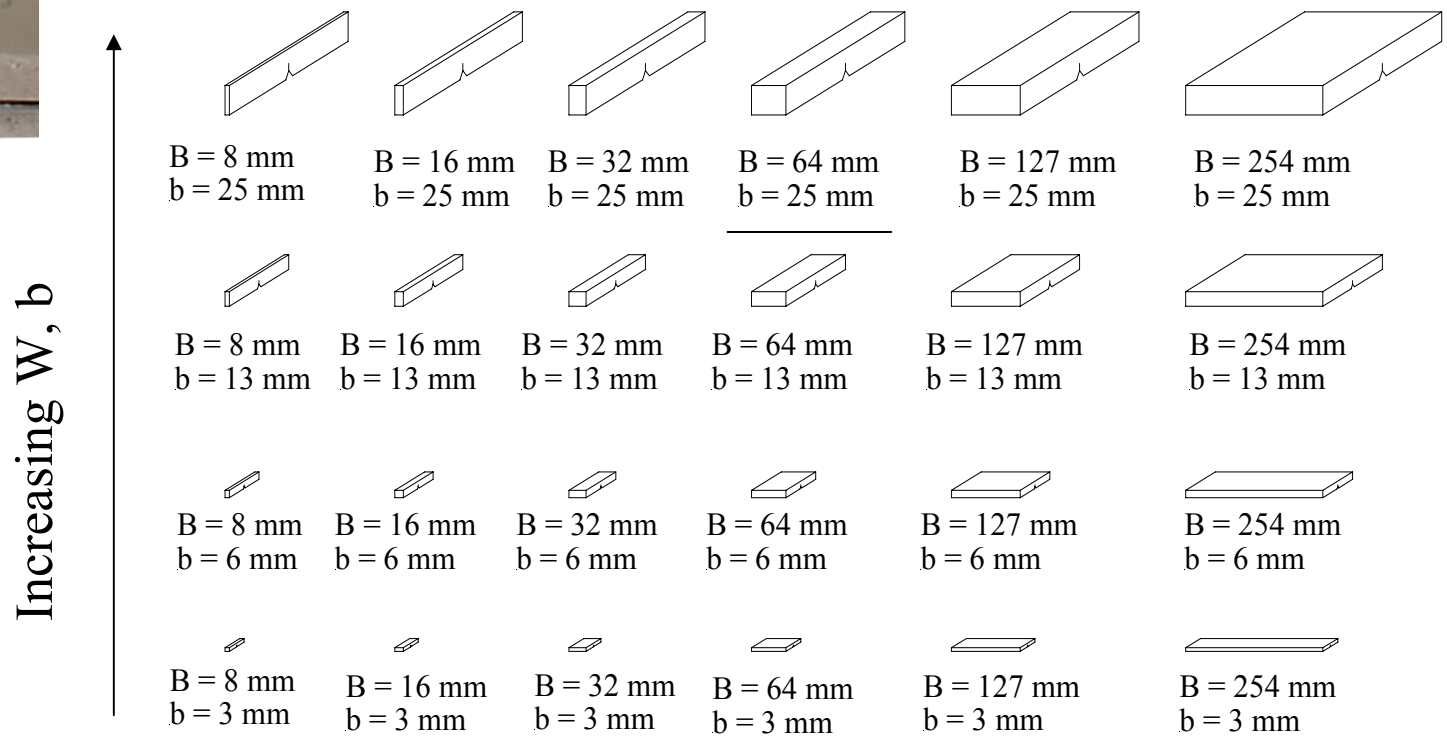

8 test per B-b

Results

- Rich K_{Jm} database with targeted effects of both CL and SSV for model based analysis.

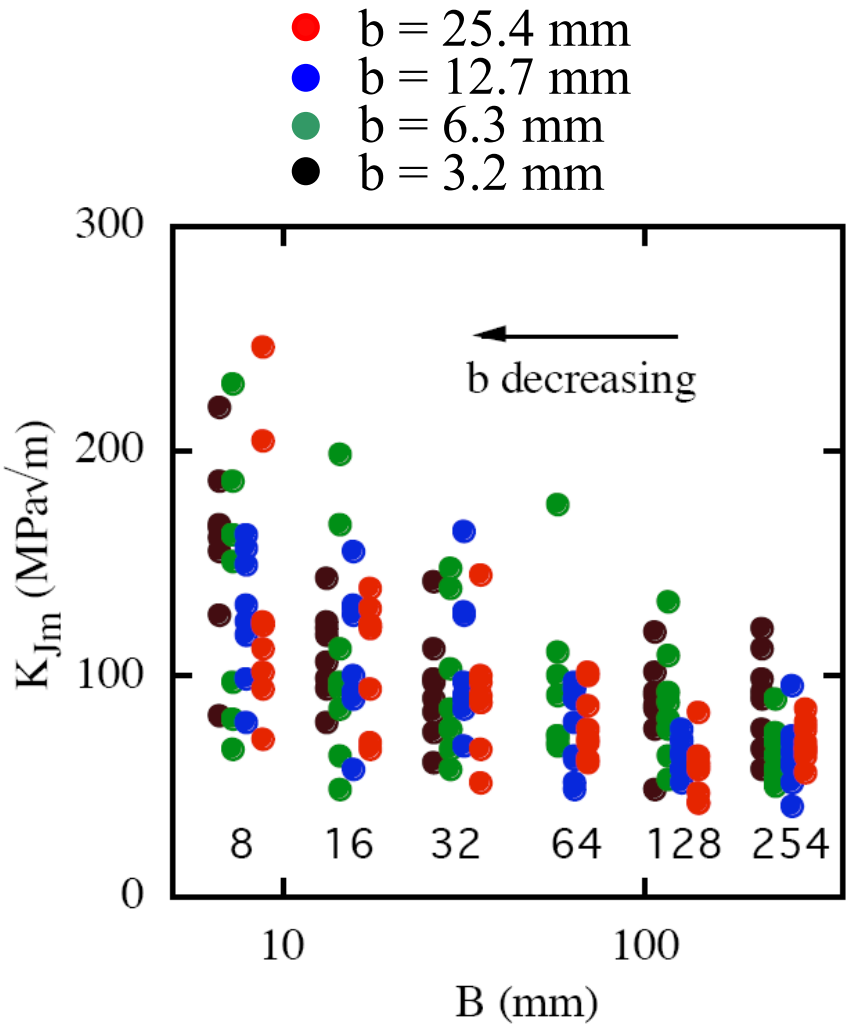

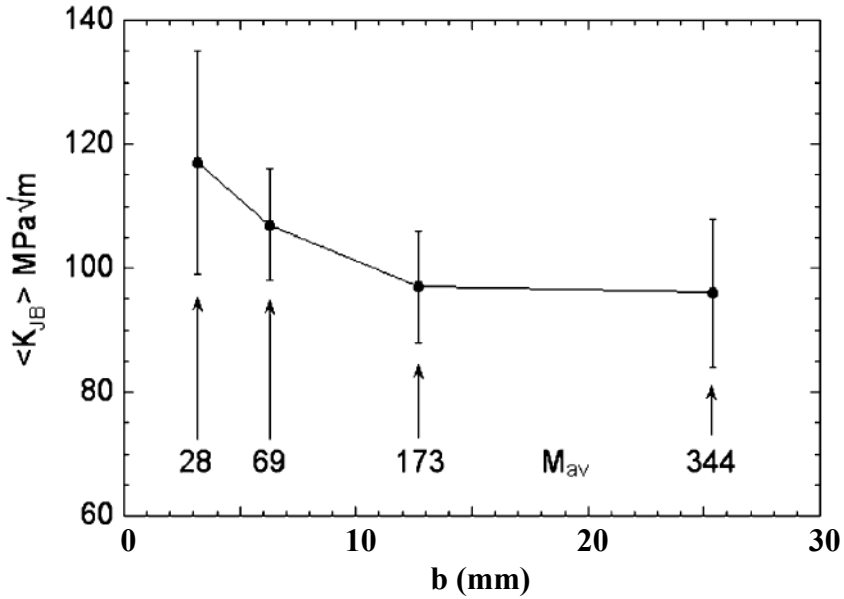

Significant constraint loss for M value greater than 30.

$K_{Jm} \Rightarrow K_{Jc} \Rightarrow K_{Jr}$ Adjustment

1. CL - FE K_{Jm}/K_{Jc} at common $A(\sigma^*)$

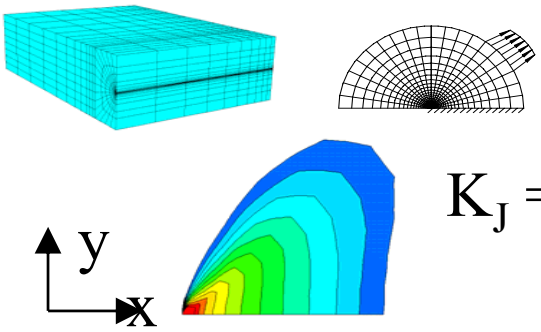

$$K_J = (E'J)^{1/2}$$

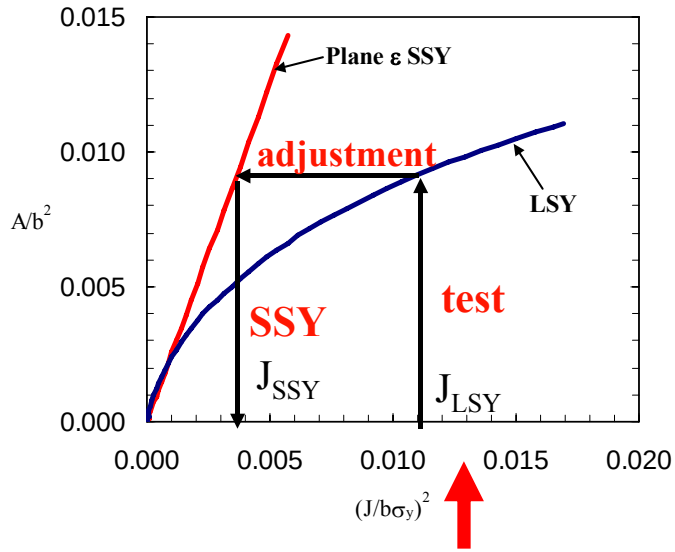

Independent calibration $\sigma^*/\sigma_y = 3$

2. Satistical

$$P_f(K_I = K_{min}) = 0$$

$$K_{Jr}(B_r) = [K_{Jc}(B) - K_{min}]\,[B/B_r]^p + K_{min}$$

ASTM E1921 ⟶ 20? 1/4?

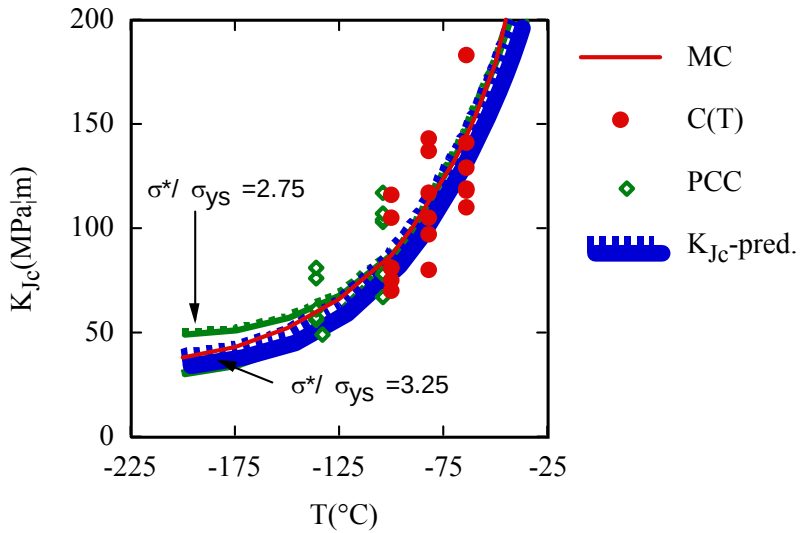

Adjusted K_{Jr}

- Approximately single K_{Jr} population within expected scatter

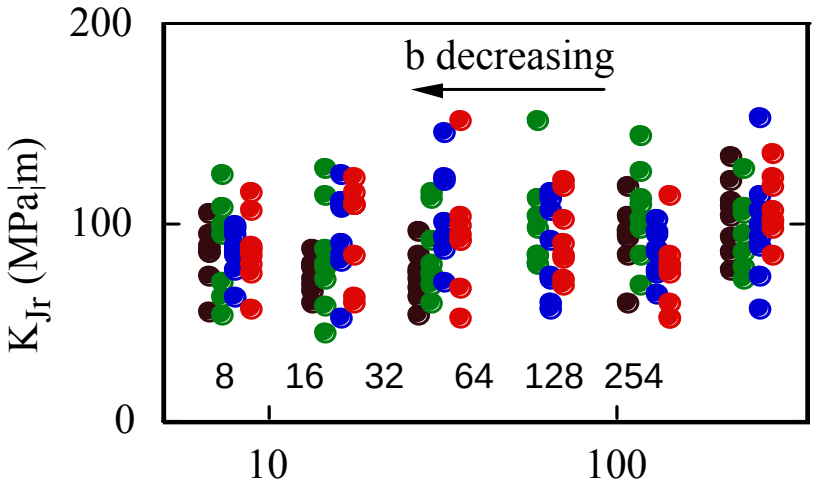

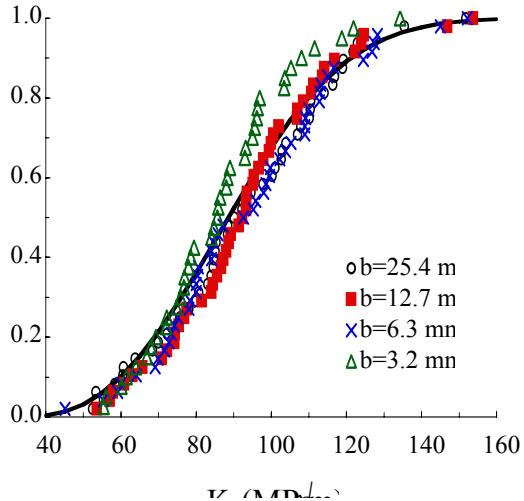

Decouple constraint loss and statistical effects

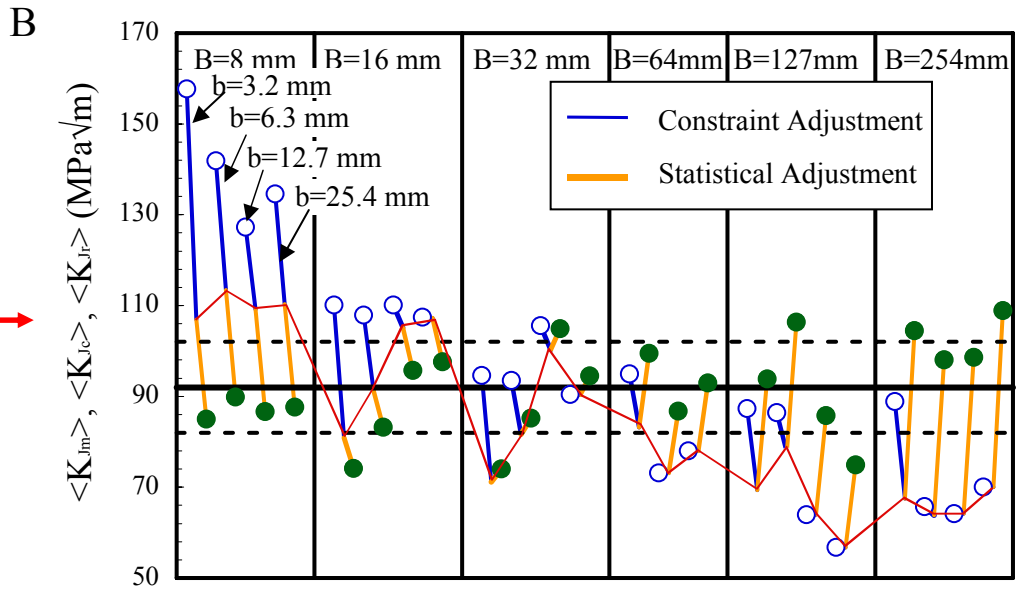

Adjusted Shoreham Database

- K_{Jm} => K_{Jr} entire Shoreham database (≈ 500 data points) => master curve T_o = -84°C

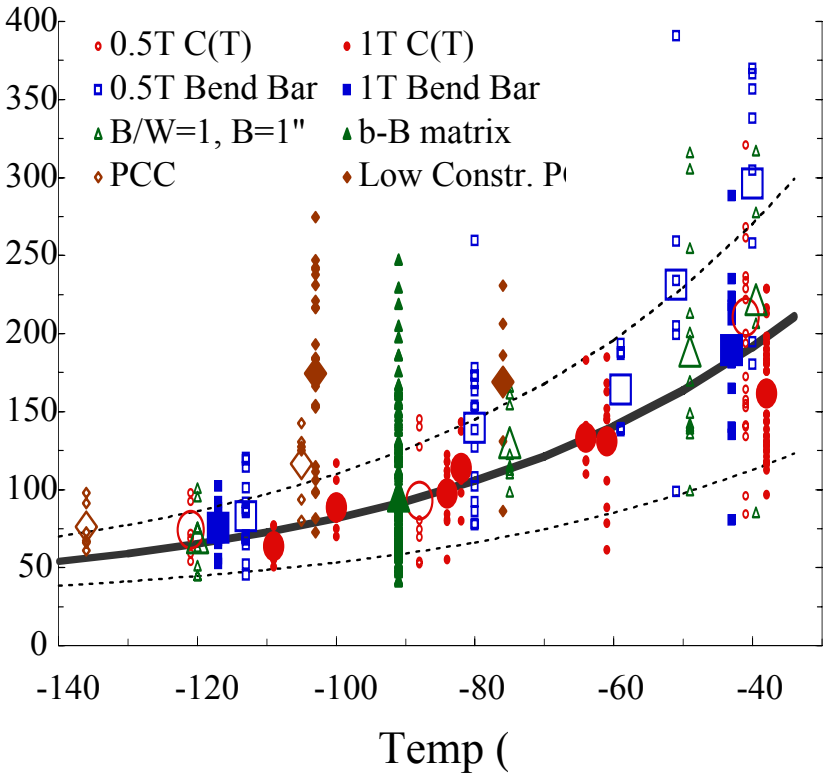

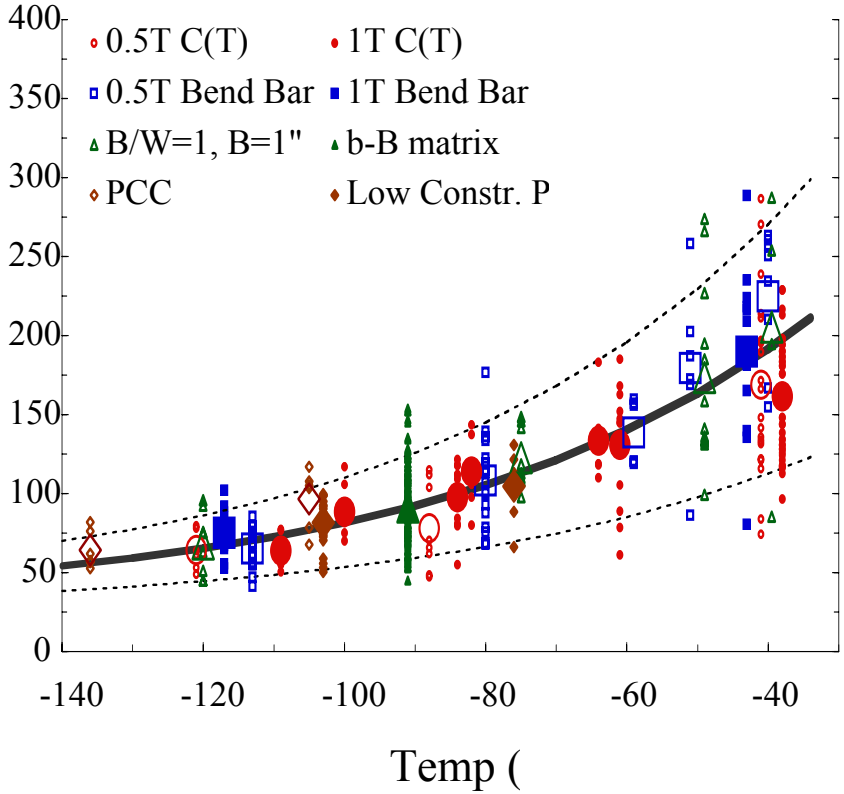

Advanced 9Cr tempered martensitic steels

- Since 80s, development of 9/12Cr TM steels within international fusion programs.
- Compositions selected to minimize the long-lived radioactive isotopes produced by neutron fusion transmutation reactions.
- Mo, Nb, Ni replaced by W, V, Mn, Ti.
- **F82H** steel (8Cr2WTa,V), IEA heat
- **Eurofer97** steel, reference steel for blanket of future fusion reactor.
- Growing fracture toughness databases analyzed according to the RPV master-curve methodology.

Toughness database in the transition F82H

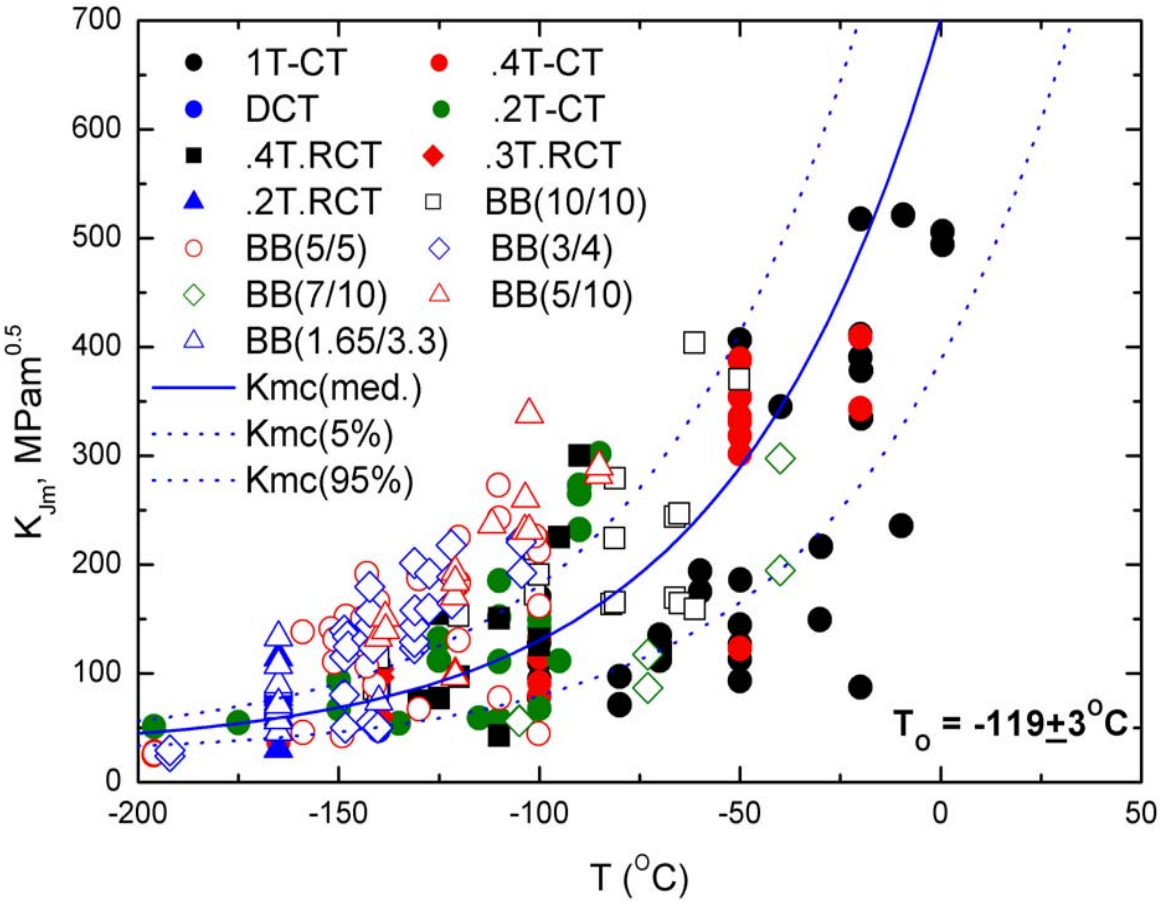

Statistical stressed volume adjusted data to 1T, without CL correction

Fully adjusted F82H database

$$K_{Jc(med)} = 30 + 70 \exp((0.019(T-T_o))$$

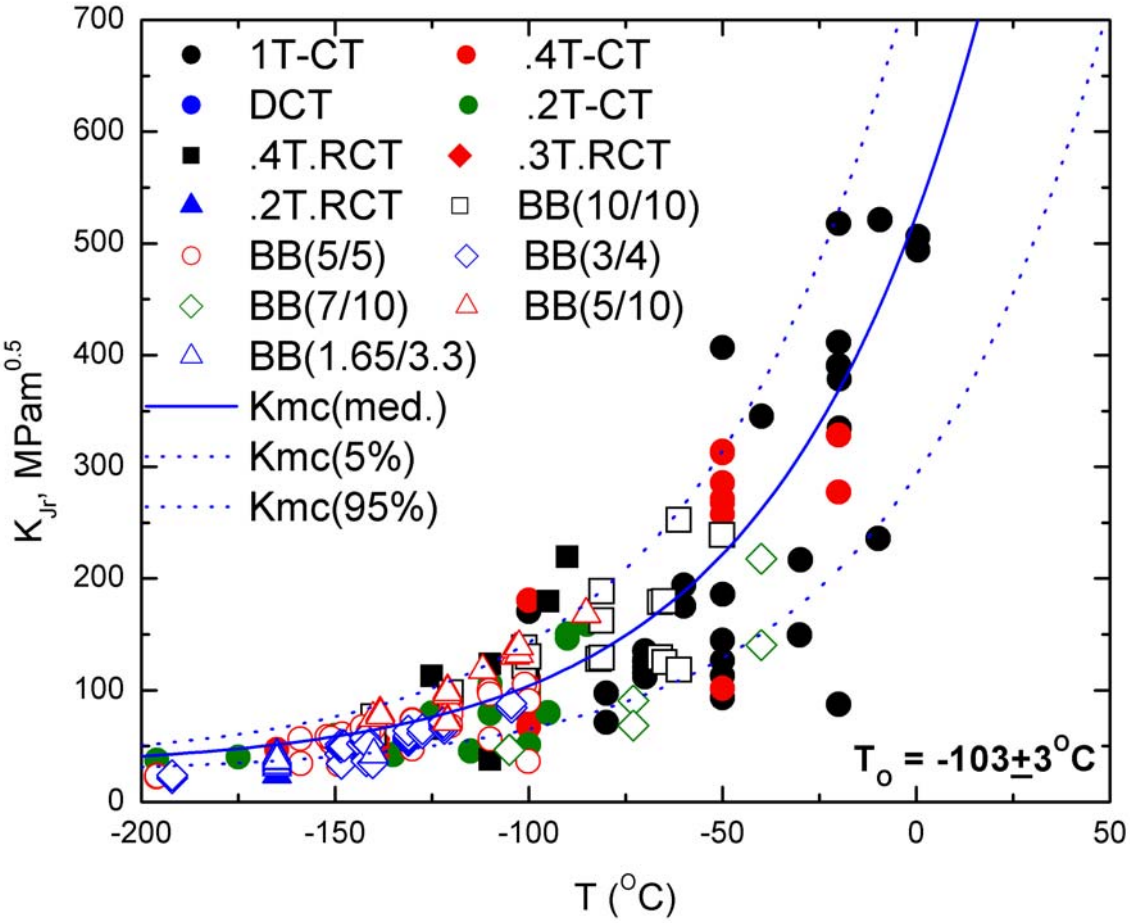

Reasonable description of the data and scatter with a RPV-Master Curve indexed at T_o=-103 °C.

Eurofer97 toughness in the transition

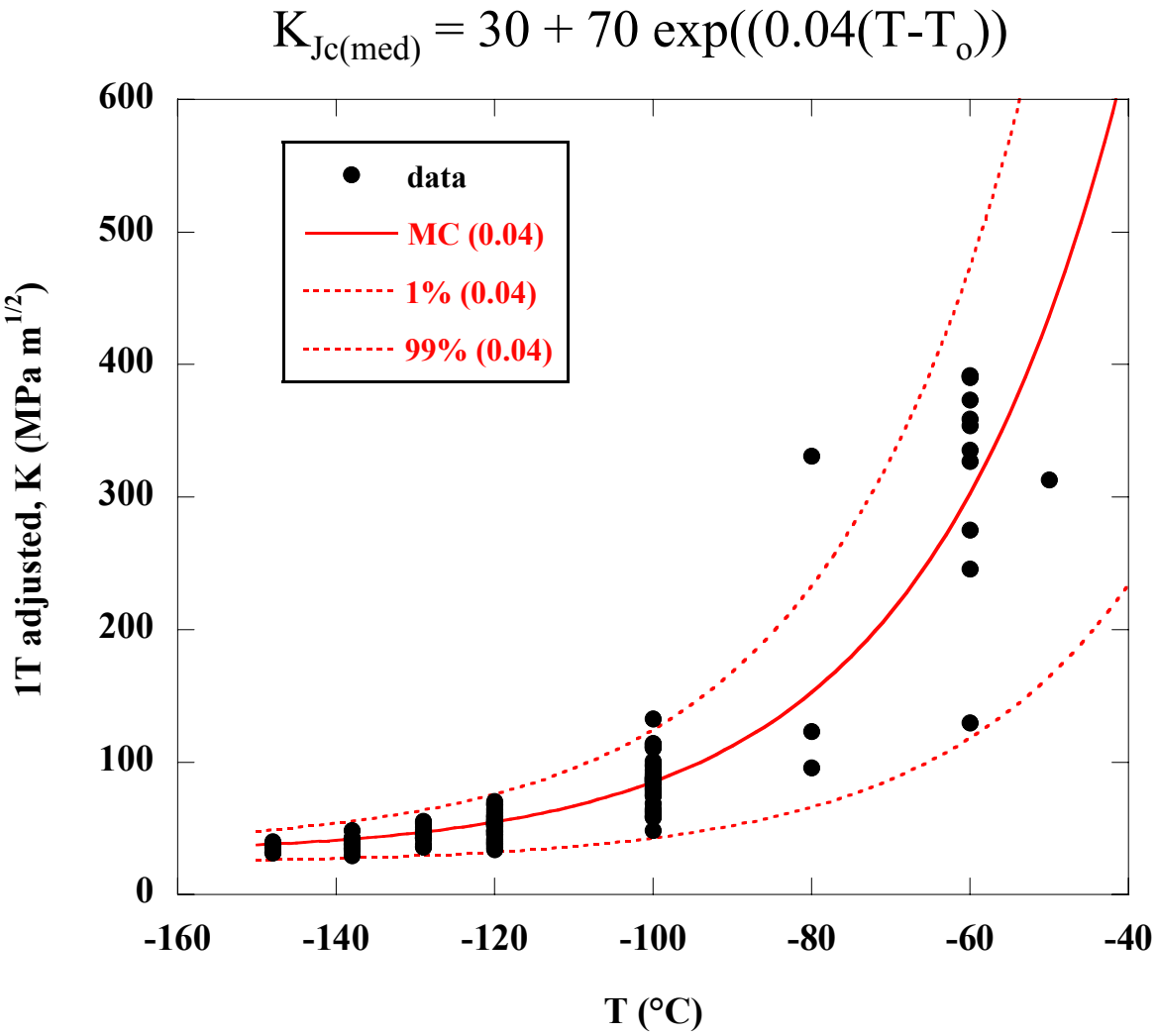

The K(T) curve appears abnormally steeper than the conventional RPV MC.

K(T) shape versus microstructure

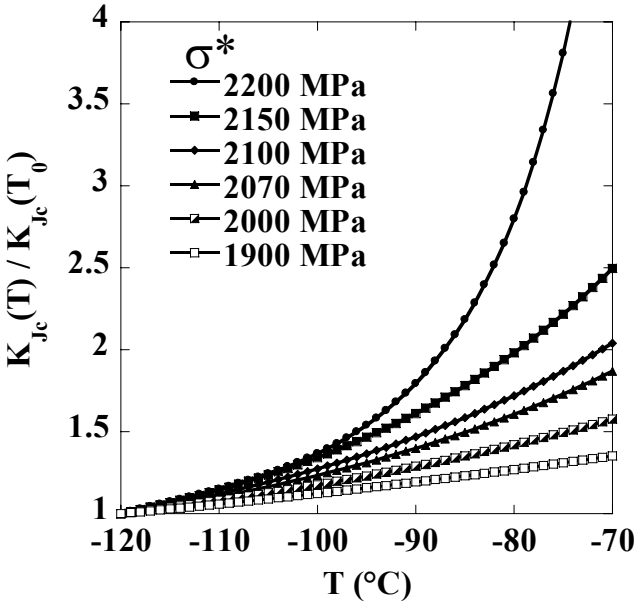

$K_{Jc(med)} = 30 + 70 \exp((\alpha(T-T_o))$

$\alpha = 0.019$ for F82H

$\alpha = 0.04$ for Eurofer97

K(T) shape mediated by σ* with:

$$\sigma^*(T) = \frac{CK_\mu(T)}{\sqrt{d}}$$

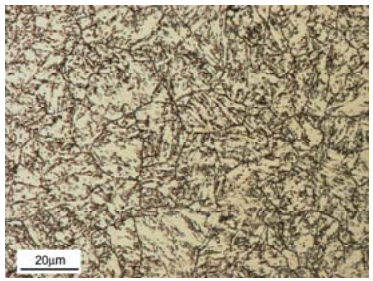

Eurofer97
PAG 10 µm

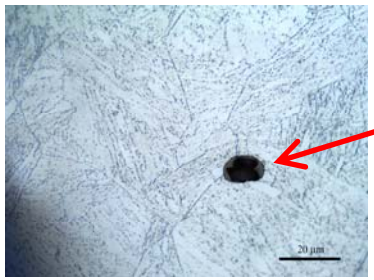

F82H
PAG 80 µm

Big inclusions >10 µm in F82H

$\sqrt{d}_{Eurofer} < \sqrt{d}_{F82H}$ or $\sigma^*_{Eurofer} > \sigma^*_{F82H}$

steeper slope for Eurofer97

Modeling the lower bound – Eurofer97

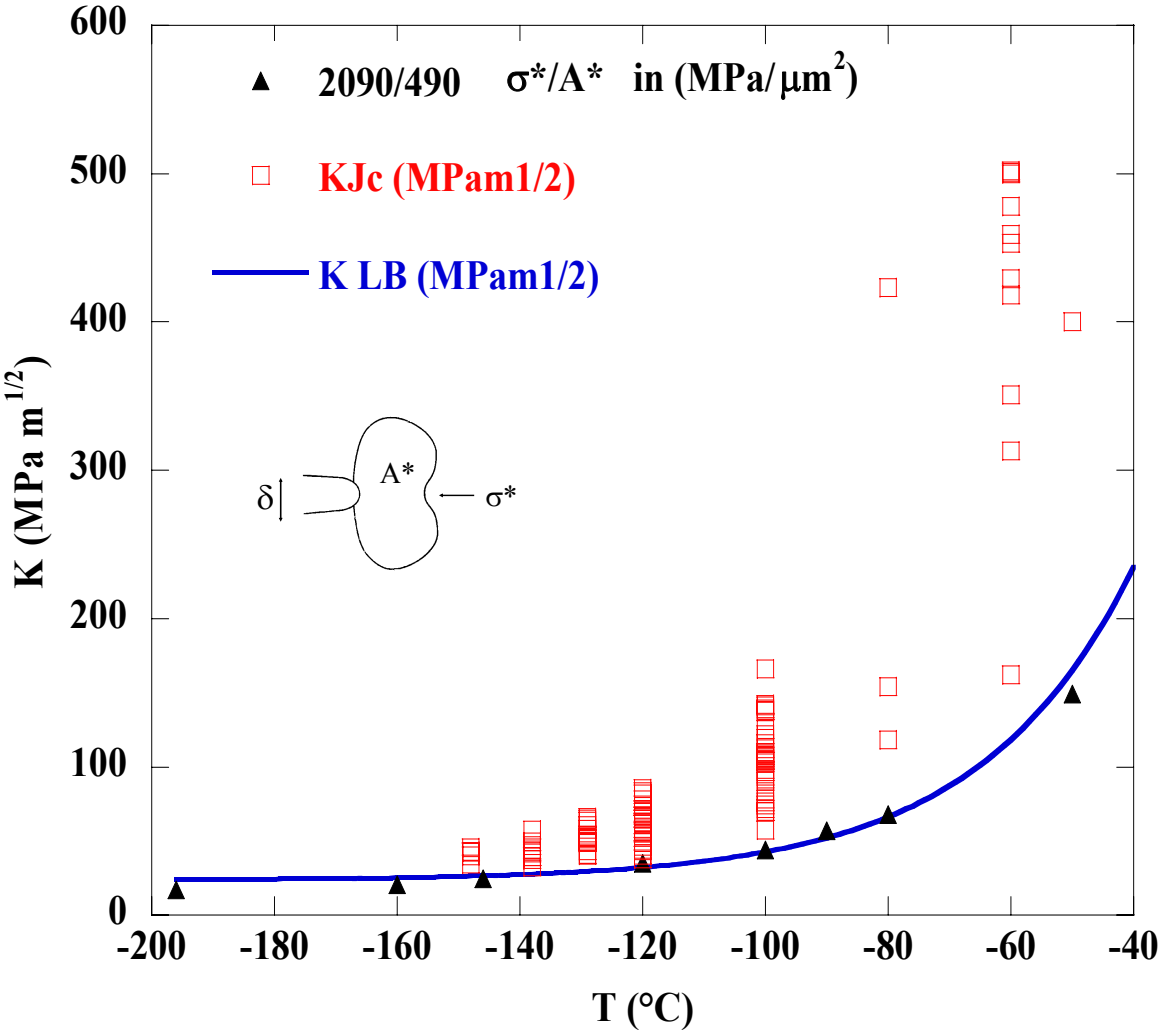

σ*-A* criterion applied to notched tensile specimens – Eurofer97.

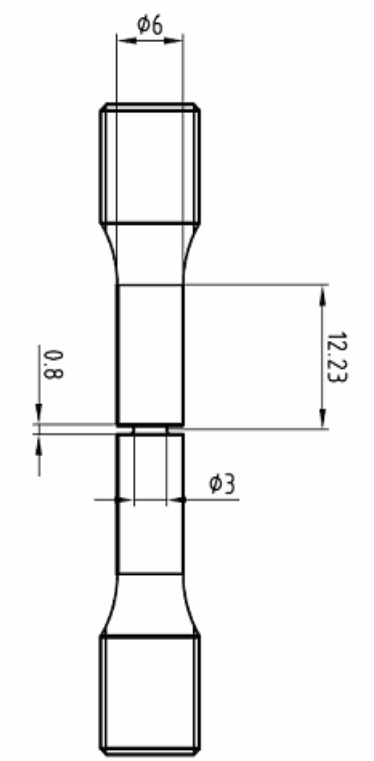

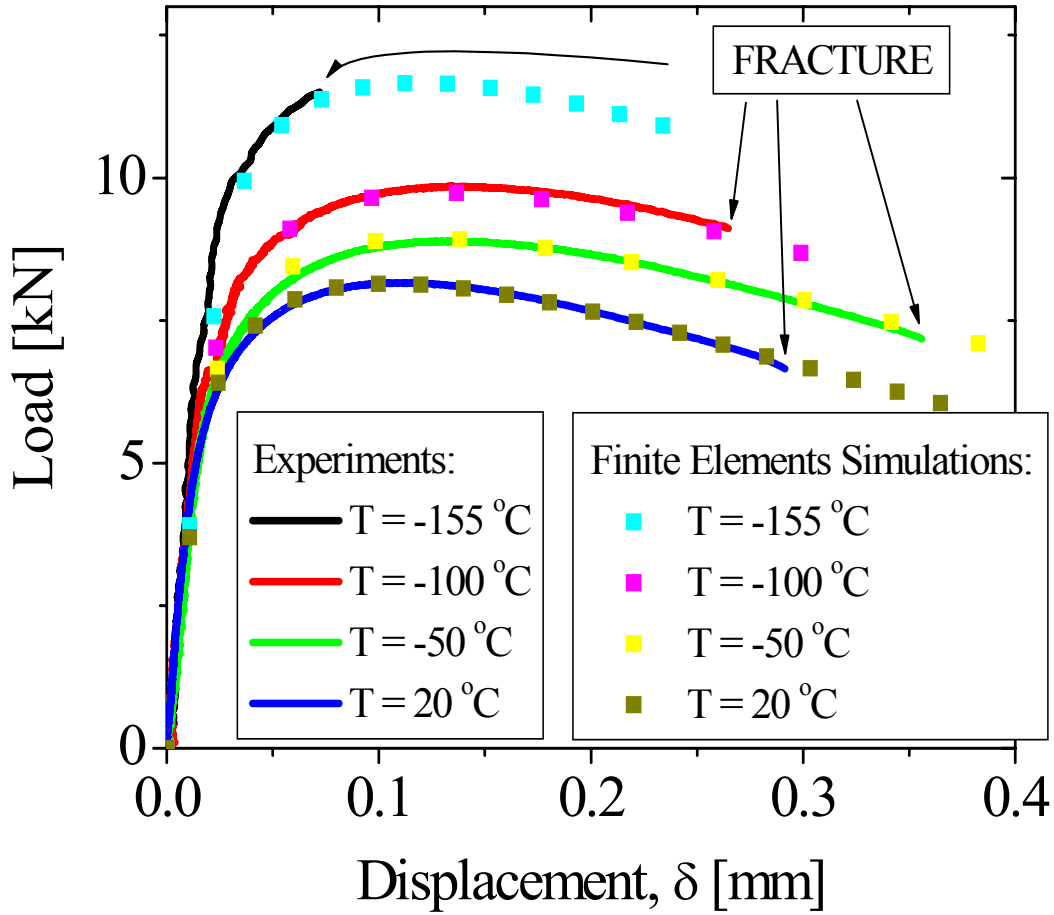

Experimental P-Δ curves and FE simulations.

Stress around the notch

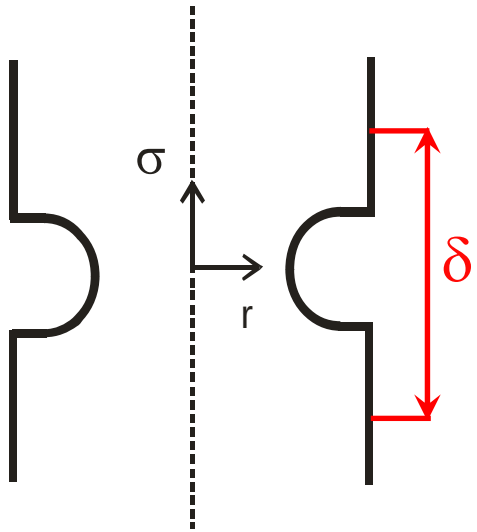

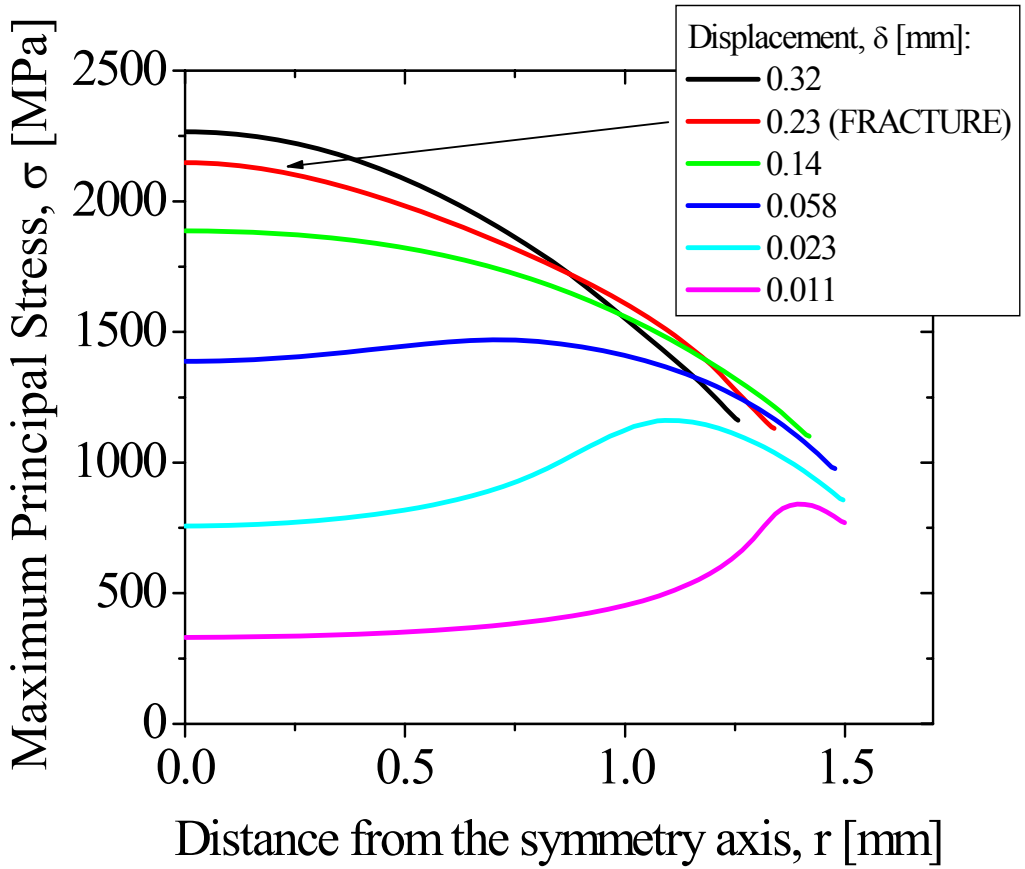

Evolution of the stress profile ahead of the notch with deformation.

Transferability of the σ*-A* criterion to notched tensile specimens.

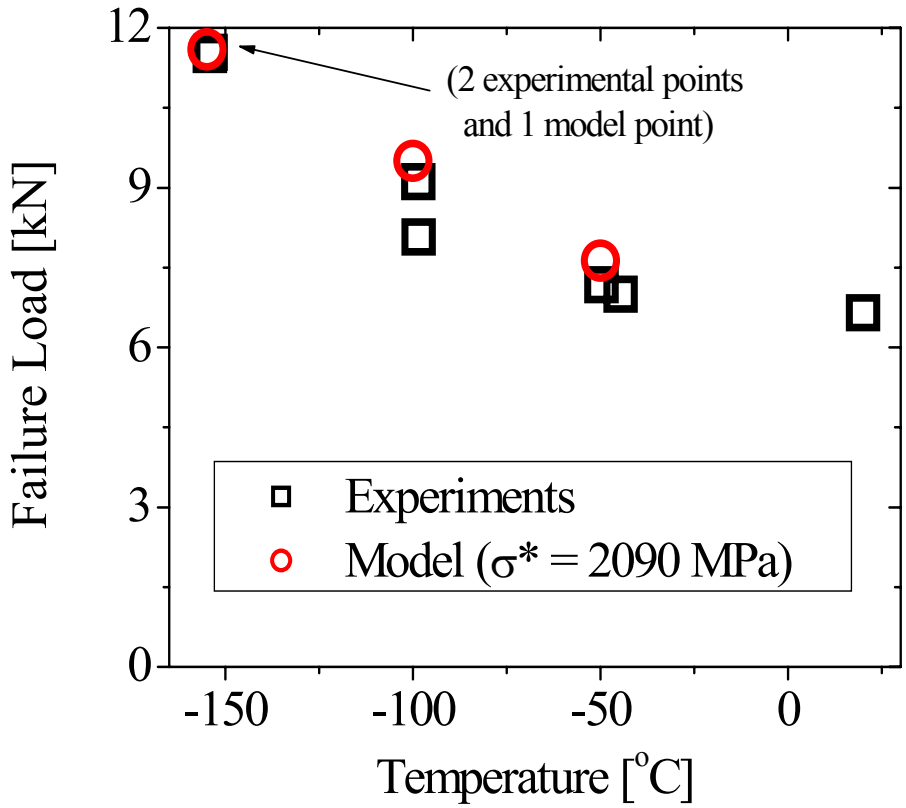

Good prediction of the load/displacement at failure based upon the σ*-A* calibrated on the pre-cracked specimens.

F82H - 60°C irradiation at 2.3 dpa

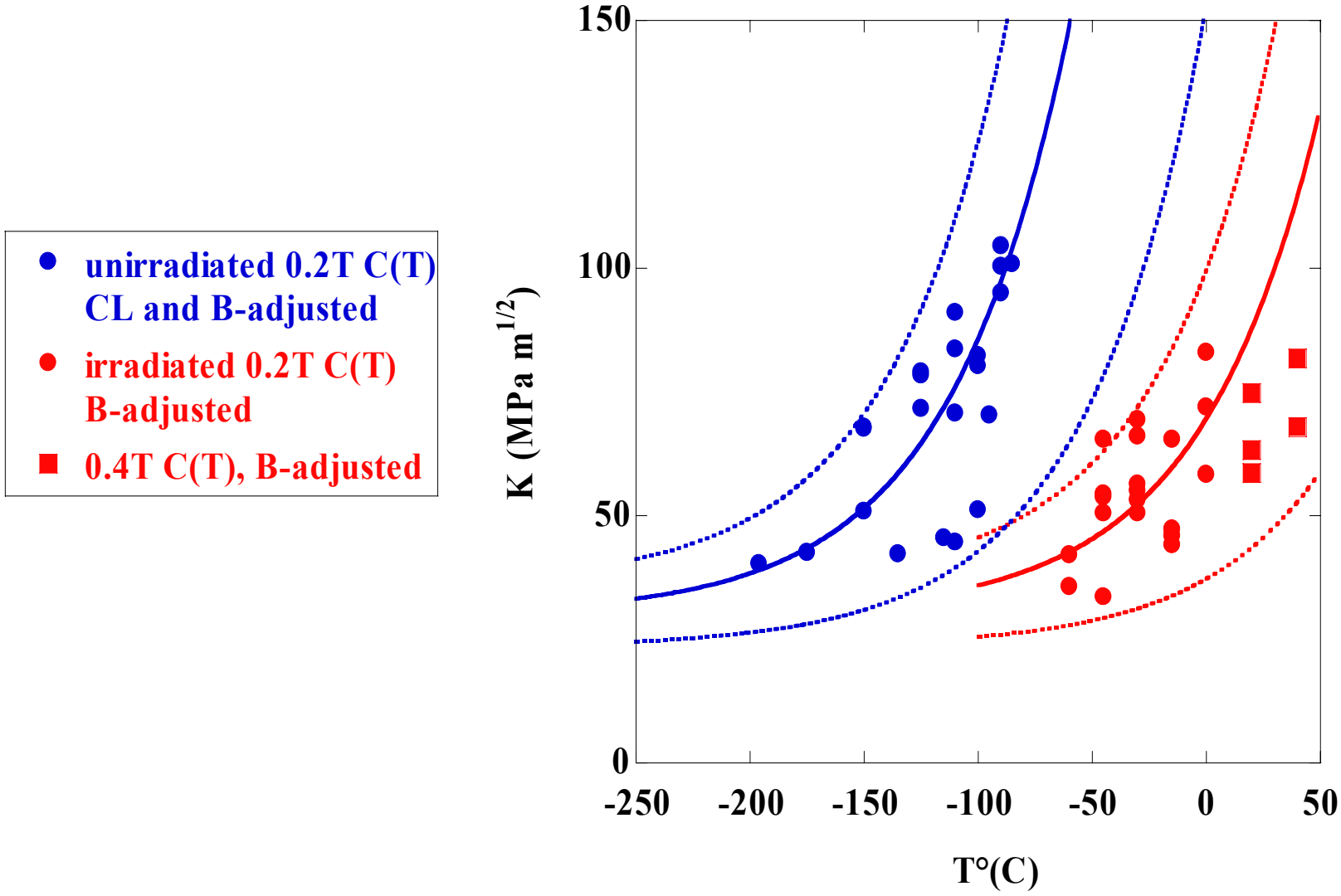

Multi-temperature T_o determination: T_o = -88°C T_o=30°C

350°C proton-irradiation at 0.5 dpa – Eurofer97

1 mm x 1 mm pre-cracked bend bar, nominal a/W=0.5, have been irradiaed with 590 MeV protons He effects studies in a 590 MeV proton spectrum.

Small mass reduces beam heating.

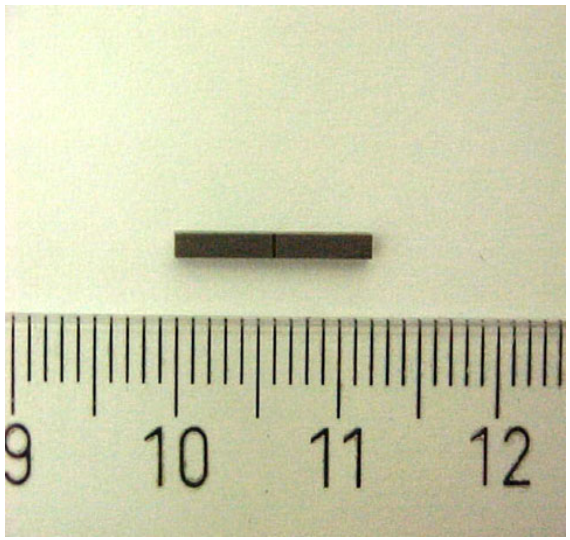

350°C proton-irradiation at 0.5 dpa – Eurfoer97

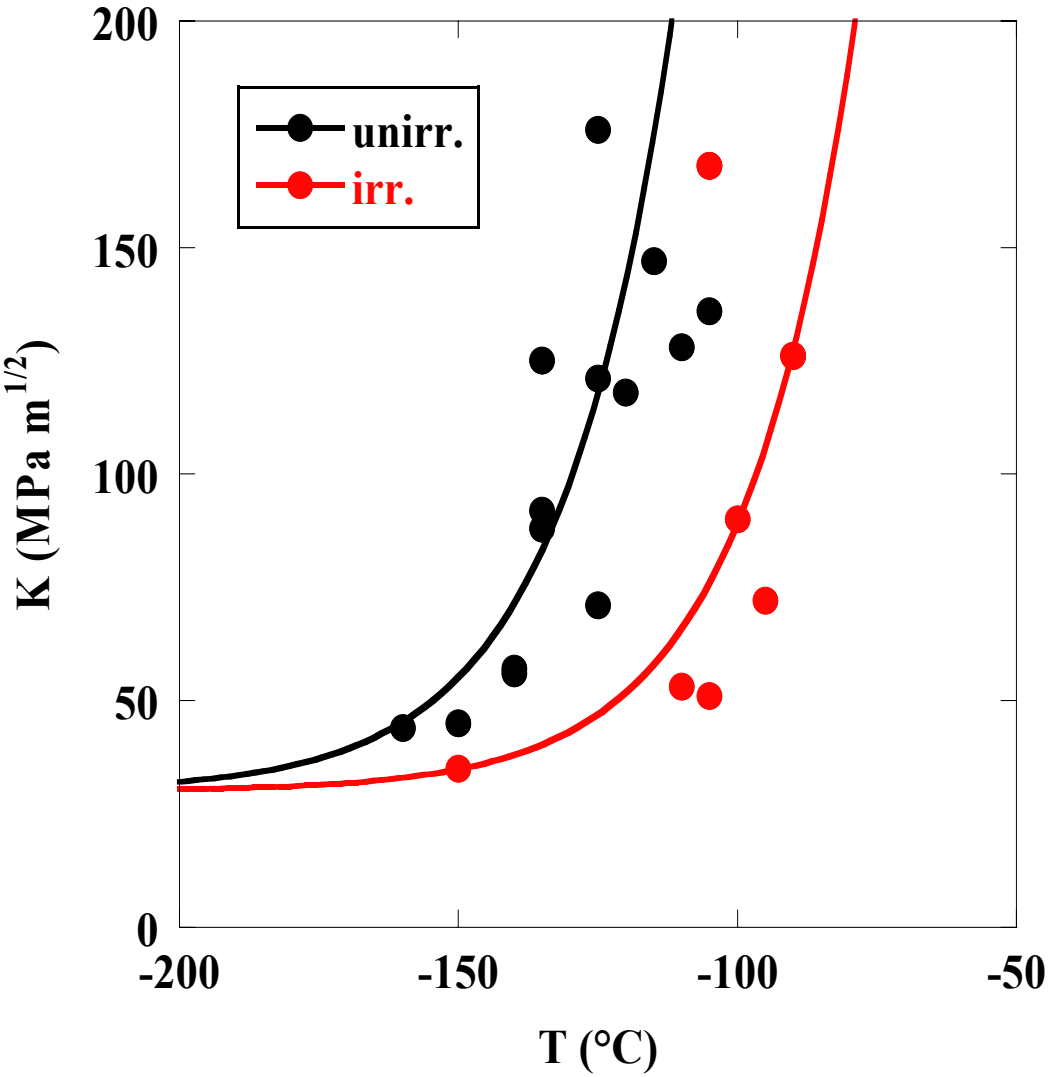

$\Delta T = 30$ °C

$\Delta\sigma_y$ - ΔT_o

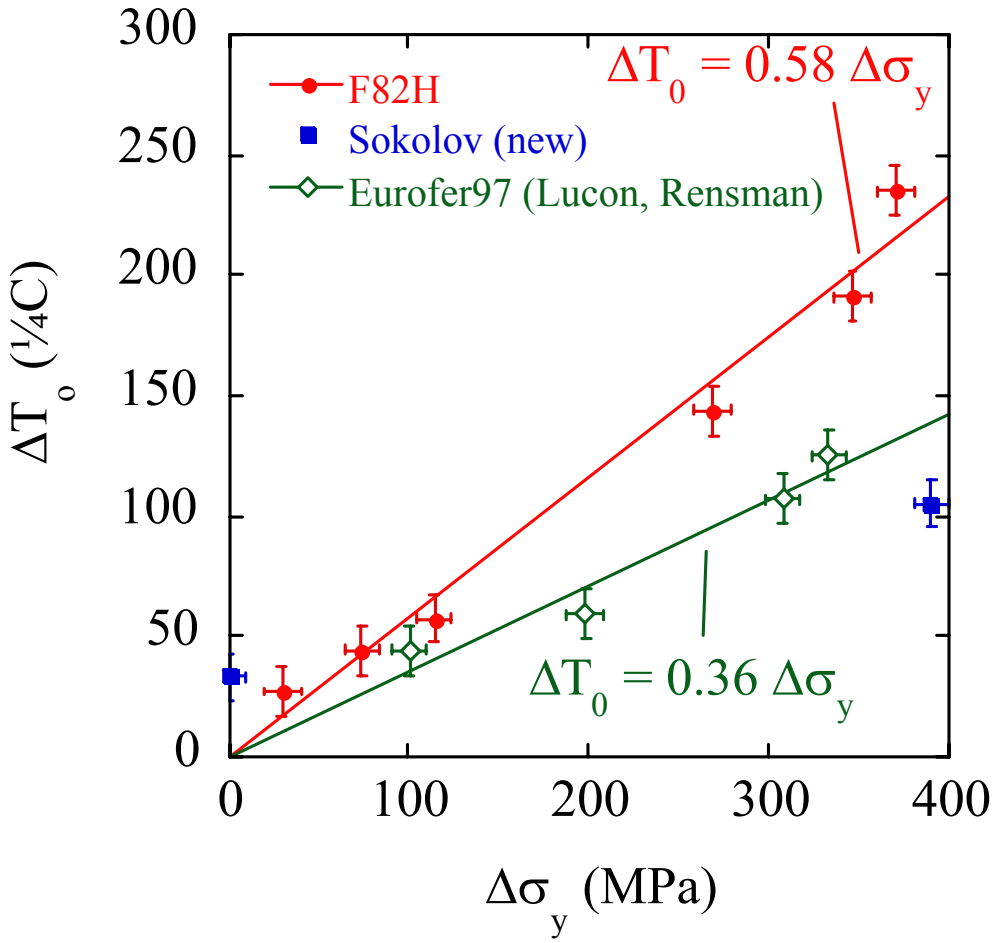

Strain Hardening Effects

- Effects of irradiation on strain hardening are important
- Minimal $\sigma_{sh}(\varepsilon)$ in low dose RPV steel irradiations: $\Delta\sigma_y \approx \Delta\sigma_{flow}$
- Large $\sigma_{sh}(\varepsilon)$ decrease/strain softening in high dose TMS alloy irradiations: $\Delta\sigma_y >> \Delta\sigma_{flow}$

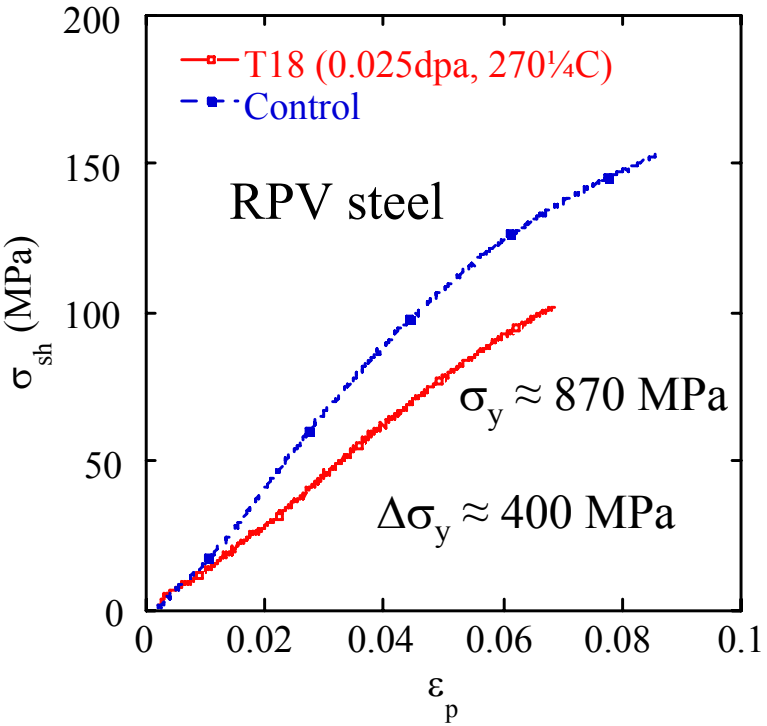

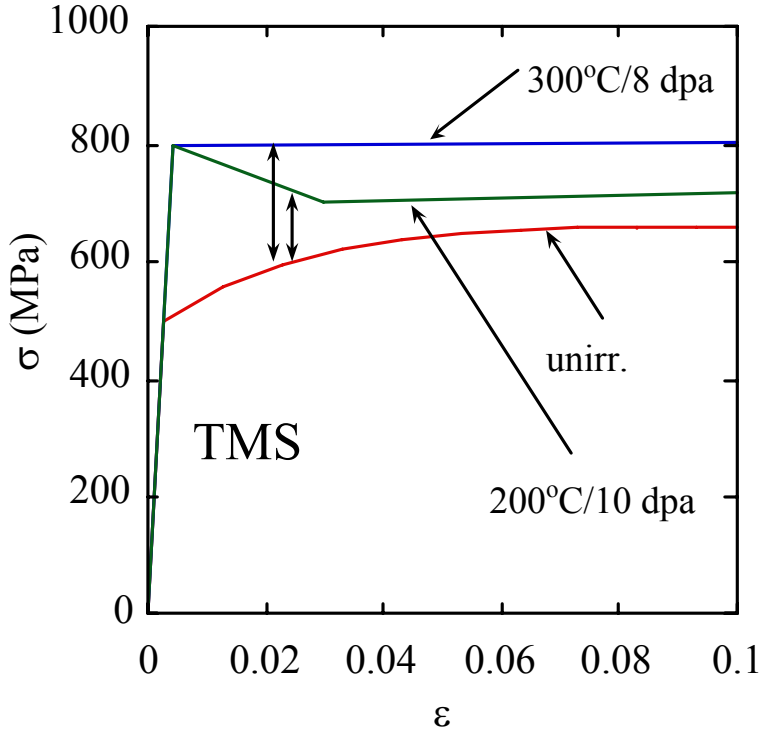

Effects of $\Delta\sigma_{sh}$ on $\Delta T_o/\Delta\sigma_y$

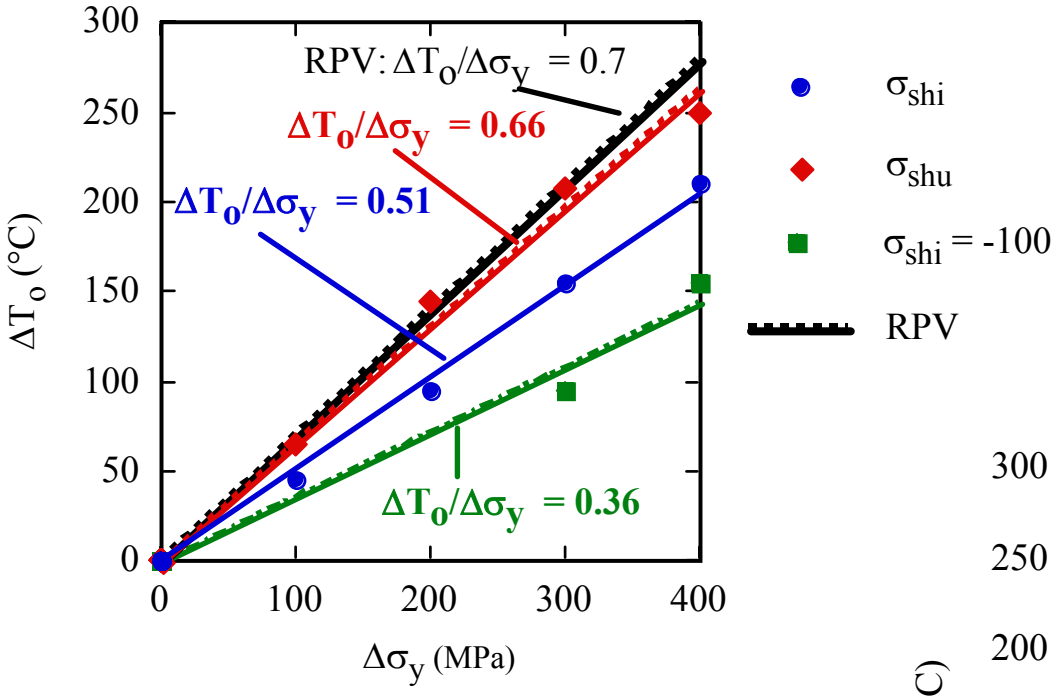

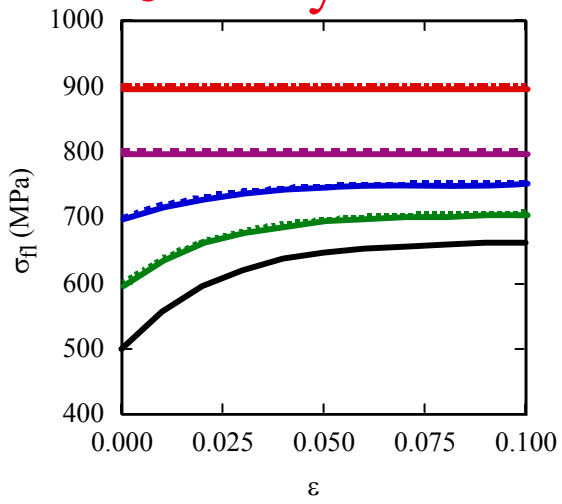

$<\sigma_{fl}> = \sigma_y + <\sigma_{sh}>$ (0-10%)

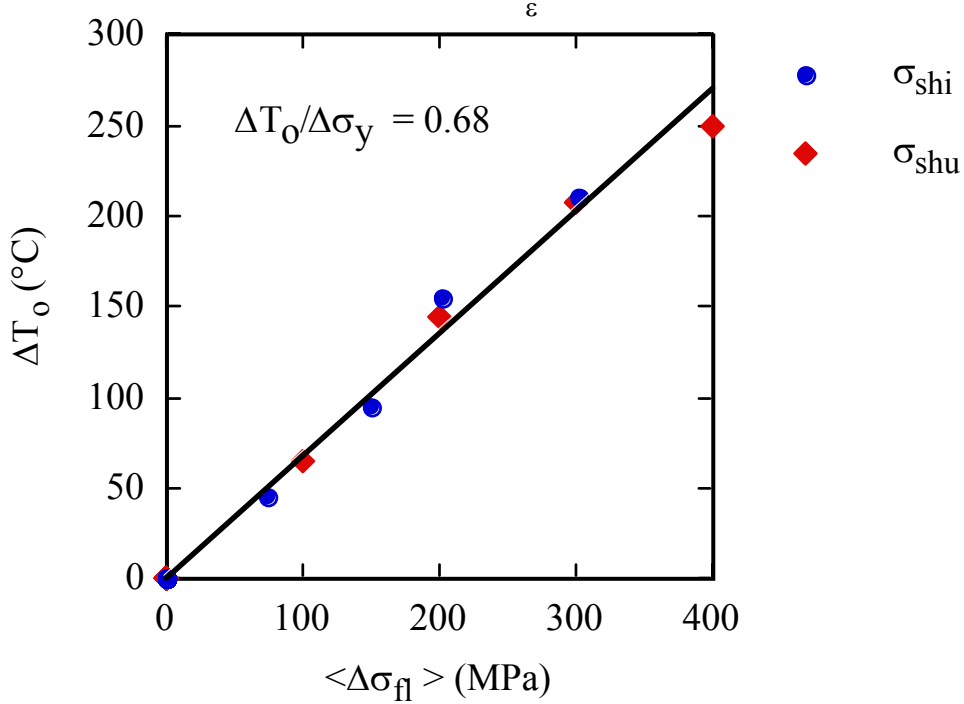

Universal Hardness Relation

- The average strain hardened flow stress from ≈ 0 to 10%ε is the best measure of local "strength" in the process zone
- FE simulations and experiments on materials with an enormous range of s(e) laws shows H also is closely related to average strain hardened flow stress from ≈ 0 to 10%ε

FE simulation

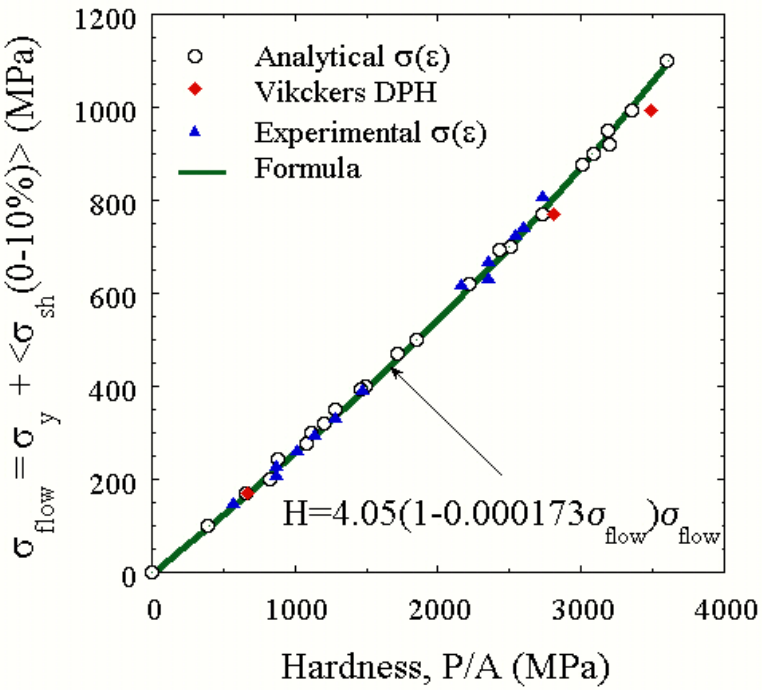

Experimental validation

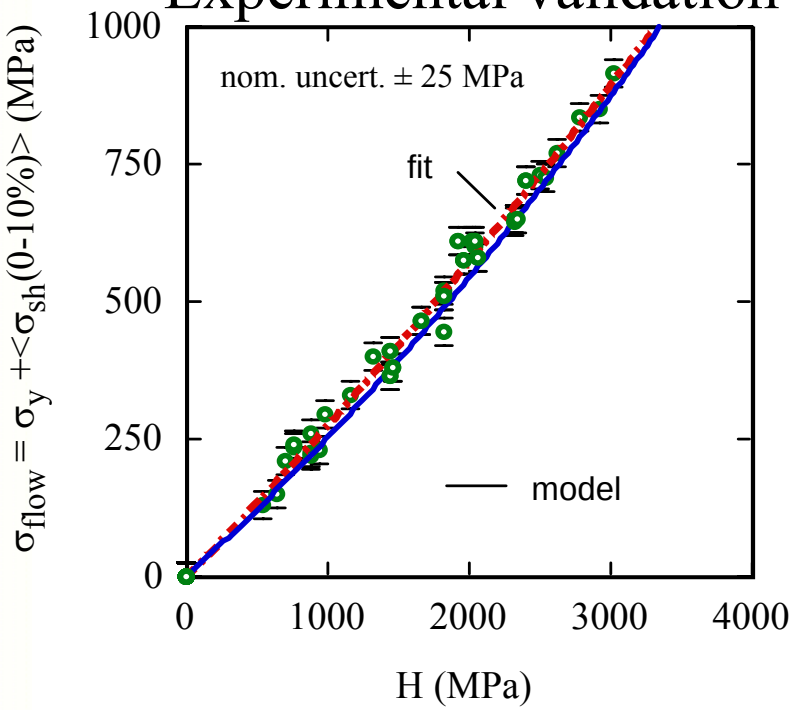

Summary

- Measured fracture toughness K_{Jm} on usual laboratory specimens is mediated by statistical and constraint loss effect associated with specimen sizes and crack length.
- The individual and coupled CL and SSV effects on K_{Jm} were discussed. K_{Jm} were adjusted to a reference K_r in SSY with a two step adjustment procedure: i) CL are first account for with a σ^*-V^* calibrated model, ii) the statistical effects are considered with a K_{min}-modifed criterion of equivalent stressed volume.
- The critical stress σ^* to propagate a microcrack scales with the arrest toughness of the ferritic matrix K_μ.
- K_μ was shown to be T-dependent with Fe single crystal initiation and arrest fracture toughness experiments.

Summary

- The dynamics of cleavage of Fe single cleavage mimics that of thermally-activated motion of dislocations.
- The K_a, hence, σ^* temperature dependence result in the approximate invariance of the MC $K_{Jc}(T-T_o)$ shape.
- Application of the master-curve methodology to advanced high-Cr tempered martensitic steels is a very promising approach.
- There are many unresolved issues including differences in the MC shape, shallow crack effects, specimen constraint-size limits especially for irradiation testing, non-hardening embrittlement including possible He effect, etc…